Local unitary transformation, long-range quantum entanglement, wave function renormalization, and topological order

PHYSICAL REVIEW B **82**, 155138 (2010)

Local unitary transformation, long-range quantum entanglement, wave function renormalization, and topological order

Xie Chen,[1] Zheng-Cheng Gu,[2] and Xiao-Gang Wen[1]
[1]*Department of Physics, Massachusetts Institute of Technology, Cambridge, Massachusetts 02139, USA*
[2]*Kavli Institute for Theoretical Physics, University of California, Santa Barbara, California 93106, USA*
(Received 28 July 2010; revised manuscript received 21 September 2010; published 26 October 2010)

Two gapped quantum ground states in the same phase are connected by an adiabatic evolution which gives rise to a local unitary transformation that maps between the states. On the other hand, gapped ground states remain within the same phase under local unitary transformations. Therefore, local unitary transformations define an equivalence relation and the equivalence classes are the universality classes that define the different phases for gapped quantum systems. Since local unitary transformations can remove local entanglement, the above equivalence/universality classes correspond to pattern of long-range entanglement, which is the essence of topological order. The local unitary transformation also allows us to define a wave function renormalization scheme, under which a wave function can flow to a simpler one within the same equivalence/universality class. Using such a setup, we find conditions on the possible fixed-point wave functions where the local unitary transformations have *finite* dimensions. The solutions of the conditions allow us to classify this type of topological orders, which generalize the string-net classification of topological orders. We also describe an algorithm of wave function renormalization induced by local unitary transformations. The algorithm allows us to calculate the flow of tensor-product wave functions which are not at the fixed points. This will allow us to calculate topological orders as well as symmetry-breaking orders in a generic tensor-product state.

DOI: 10.1103/PhysRevB.82.155138 PACS number(s): 64.70.Tg, 71.27.+a

I. INTRODUCTION

According to the principle of emergence, the rich properties and the many different forms of materials originate from the different ways in which the atoms are ordered in the materials. Landau symmetry-breaking (SB) theory provides a general understanding of those different orders and resulting rich states of matter.[1,2] It points out that different orders really correspond to different symmetries in the organizations of the constituent atoms. As a material changes from one order to another order (i.e., as the material undergoes a phase transition), what happens is that the symmetry of the organization of the atoms changes.

For a long time, we believed that Landau symmetry-breaking theory describes all possible orders in materials and all possible (continuous) phase transitions. However, in last 20 years, it has become more and more clear that Landau symmetry-breaking theory does not describe all possible orders. After the discovery of high-T_c superconductors in 1986,[3] some theorists believed that quantum spin liquids play a key role in understanding high-T_c superconductors[4] and started to introduce various spin liquids.[5–9] Despite the success of Landau symmetry-breaking theory in describing all kinds of states, the theory cannot explain and does not even allow the existence of spin liquids. This leads many theorists to doubt the very existence of spin liquids. In 1987, in an attempt to explain high-temperature superconductivity, an infrared stable spin liquid—chiral spin state was discovered,[10,11] which was shown to be perturbatively stable and exist as quantum phase of matter (at least in a large N limit). At first, not believing Landau symmetry-breaking theory fails to describe spin liquids, people still wanted to use symmetry breaking to describe the chiral spin state. They identified the chiral spin state as a state that breaks the time-reversal and parity symmetries but not the spin rotation symmetry.[11] However, it was quickly realized that there are many different chiral spin states that have exactly the same symmetry, so symmetry alone is not enough to characterize different chiral spin states. This means that the chiral spin states contain a new kind of order that is beyond symmetry description.[12] This new kind of order was named[13] topological order.[14]

The key to identify (and define) new orders is to identify new universal properties that are beyond the local order parameters and long-range correlations used in the Landau symmetry-breaking theory. Indeed, new quantum numbers, such as ground-state degeneracy,[12] the non-Abelian Berry's phase of degenerate ground states,[13] and edge excitations,[15] were introduced to characterize (and define) the different topological orders in chiral spin states. Recently, it was shown that topological orders can also be characterized by topological entanglement entropy.[16,17] More importantly, those quantities were shown to be universal (i.e., robust against any local perturbation of the Hamiltonian) for chiral spin states.[13] The existence of those universal properties establishes the existence of topological order in chiral spin states.

Near the end of 1980s, the existence of chiral spin states as a theoretical possibility, as well as their many amazing properties, such as fractional statistics,[10,11] spin-charge separation,[10,11] and chiral gapless edge excitations,[15] were established reliably, at least in the large N limit introduced in Ref. 18. Even non-Abelian chiral spin states can be established reliably in the large N limit.[19] However, it took about 10 years to establish the existence of a chiral spin state reliably without using large N limit (based on an exactly soluble model on honeycomb lattice).[20]

Soon after the introduction of chiral spin states, experiments indicated that high-temperature superconductors do

not break the time-reversal and parity symmetries. So chiral spin states do not describe high-temperature superconductors. Thus the theory of topological order became a theory with no experimental realization. However, the similarity between chiral spin states and fractional quantum Hall (FQH) states allows one to use the theory of topological order to describe different FQH states.[21] Just like chiral spin states, different FQH states all have the same symmetry and are beyond the Landau symmetry-breaking description. Also like chiral spin states, FQH states have ground-state degeneracies[22] that depend on the topology of the space.[13,21] Those ground-state degeneracies are shown to be robust against any perturbations. Thus, the different orders in different quantum Hall states can be described by topological orders, and the topological order does have experimental realizations.

The topology-dependent ground-state degeneracy, that signal the presence of topological order, is an amazing phenomenon. In FQH states, the correlation of any local operators are short ranged. This seems to imply that FQH states are "short sighted" and they cannot know the topology of space which is a global and long-distance property. However, the fact that ground-state degeneracy does depend on the topology of space implies that FQH states are not short sighted and they do find a way to know the global and long-distance structure of space. So, despite the short-range correlations of any local operators, the FQH states must contain certain hidden long-range correlation. But what is this hidden long-range correlation? This will be one of the main topic of this paper.

Since high-T_c superconductors do not break the time-reversal and parity symmetries, nor any other lattice symmetries, some people concentrated on finding spin liquids that respect all those symmetries and hoping one of those symmetric spin liquids hold the key to understand high-T_c superconductors. Between 1987 and 1992, many symmetric spin liquids were introduced and studied.[5–9,23–26] The excitations in some of constructed spin liquids have a finite energy gap while in others there is no energy gap. Those symmetric spin liquids do not break any symmetry and, by definition, are beyond Landau symmetry-breaking description.

By construction, topological order only describes the organization of particles or spins in a gapped quantum state. So the theory of topological order only applies to gapped spin liquids. Indeed, we find that the gapped spin liquids do contain nontrivial topological orders[25] (as signified by their topology-dependent and robust ground-state degeneracies) and are described by topological quantum field theory (such as $\mathbb{Z}_2$ gauge theory) at low energies. One of the simplest topologically ordered spin liquids is the $\mathbb{Z}_2$ spin liquid which was first introduced in 1991.[24,25] The existence of $\mathbb{Z}_2$ spin liquid as a theoretical possibility, as well as its many amazing properties, such as spin-charge separation,[24,25] fractional mutual statistics,[25] and topologically protected ground-state degeneracy,[25] were established reliably (at least in the large N limit introduced in Ref. 18). Later, Kitaev introduced the famous toric code model which establishes the existence of the $\mathbb{Z}_2$ spin liquid reliably without using large N limit.[27] The topologically protected degeneracy of the $\mathbb{Z}_2$ spin liquid was used to perform fault-tolerant quantum computation.

The study of high-T_c superconductors also leads to many gapless spin liquids. The stability and the existence of those gapless spin liquid were in more doubts than their gapped counterparts. But careful analysis in certain large N limit do suggest that stable gapless spin liquids can exist.[18,28,29] If we do believe in the existence of gapless spin liquids, then the next question is how to describe the orders (i.e., the organizations of spins) in those gapless spin liquids. If gapped quantum state can contain new type of orders that are beyond Landau's symmetry-breaking description, it is natural to expect that gapless quantum states can also contain new type of orders. But how to show the existence of new orders in gapless states?

Just like topological order, the key to identify new orders is to identify new universal properties that are beyond Landau symmetry description. Clearly we can no longer use the ground-state degeneracy to establish the existence of new orders in gapless states. To show the existence of new orders in gapless states, a new universal quantity—projective symmetry group (PSG)—was introduced.[30] It was argued that (some) PSGs are robust against any local perturbations of the Hamiltonian that do not change the symmetry of the Hamiltonian.[28–31] So through PSG, we establish the existence of new orders even in gapless states. The new orders are called quantum order to indicate that the new orders are related to patterns of quantum entanglement in the many-body ground state.[32]

II. SHORT-RANGE AND LONG-RANGE QUANTUM ENTANGLEMENTS

What is missed in Landau theory so that it fails to describe those new orders? What is the new feature in the organization of particles/spins so that the resulting order cannot be described by symmetry?

To answer those questions, let us consider a simple quantum system which can be described with Landau theory—the transverse field Ising model in two dimensions: $H=-B\Sigma X_i - J\Sigma Z_i Z_j$, where X_i, Y_i, and Z_i are the Pauli matrices on site $\boldsymbol{i}$. In $B \gg J$ limit, the ground state of the system is an equal-weight superposition of all possible spin-up and spin-down states: $|\Phi^+\rangle = \Sigma_{\{\sigma_i\}} |\{\sigma_i\}\rangle$, where $\{\sigma_i\}$ label a particular spin-up ($Z_i=1$) and spin-down ($Z_i=-1$) configurations. In the $J \gg B$ limit, the system has two degenerate ground states $|\Phi^\uparrow\rangle = |\uparrow\uparrow\cdots\uparrow\rangle$ and $|\Phi^\downarrow\rangle = |\downarrow\downarrow\cdots\downarrow\rangle$.

The transverse field Ising model has a $Z \to -Z$ symmetry. The ground state $|\Phi^+\rangle$ respect such a symmetry while the ground state $|\Phi^\uparrow\rangle$ (or $|\Phi^\downarrow\rangle$) break the symmetry. Thus the small J ground state $|\Phi^+\rangle$ and the small B ground state $|\Phi^\uparrow\rangle$ describe different phases since they have different symmetries.

We note that $|\Phi^\uparrow\rangle$ is the exact ground state of the transverse field Ising model with $B=0$. The state has no quantum entanglement since $|\Phi^\uparrow\rangle$ is a direct product of local states: $|\Phi^\uparrow\rangle = \otimes_i |\uparrow\rangle_i$ where $|\uparrow\rangle_i$ is an up-spin state at site $\boldsymbol{i}$. The state $|\Phi^+\rangle$ is the exact ground state of the transverse field Ising model with $J=0$. It is also a state with no quantum entanglement: $|\Phi^+\rangle = \otimes_i (|\uparrow\rangle_i + |\downarrow\rangle_i) \propto \otimes_i |+\rangle_i$, where $|+\rangle_i \equiv |\uparrow\rangle_i + |\downarrow\rangle_i$ is a state with spin in x direction at site $\boldsymbol{i}$.

We see that the states (or phases) described by Landau symmetry-breaking theory has no quantum entanglement at least in the $J=0$ or $B=0$ limits. In the $J/B \ll 1$ and $B/J \ll 1$ limits, the two ground states of the two limits still represent two phases with different symmetries. However, in this case, the ground states are not unentangled. On the other hand since the ground states in the $J=0$ or $B=0$ limits have finite energy gaps and short-range correlations, a small J or a small B can only modify the states locally. Thus we expect the ground states have only short-range entanglement.

The above example, if generalized to other symmetry-breaking states, suggests the following conjecture: *if a gapped quantum ground state is described by Landau symmetry-breaking theory, then it has short-range quantum entanglement*.[33]

The direct-product states and short-range-entangled (SRE) states only represent a small subset of all possible quantum many-body states. Thus, according to the point of view of the above conjecture, we see that what is missed by Landau symmetry-breaking theory is long-range quantum entanglement. It is this long-range quantum entanglement that makes a state to have nontrivial topological/quantum order.

However, mathematically speaking, the above conjecture is a null statement since the meaning of short-range quantum entanglement is not defined. In the following, we will try to find a more precise description (or definition) of short-range and long-range quantum entanglements. We will start with a careful discussion of quantum phases and quantum phase transitions.

III. QUANTUM PHASES AND LOCAL UNITARY EVOLUTIONS

To give a precise definition of quantum phases, let us consider a local quantum system whose Hamiltonian has a smooth dependence on a parameter g: $H(g)$. The ground-state average of a local operator O of the system, $\langle O\rangle(g)$, naturally also depend on g. If the function $\langle O\rangle(g)$, in the limit of infinite system size, has a singularity at g_c for some local operators O, then the system described by $H(g)$ has a quantum phase transition at g_c. After defining phase transition, we can define when two quantum ground states belong to the same phase: let $|\Phi(0)\rangle$ be the ground state of $H(0)$ and $|\Phi(1)\rangle$ be the ground state of $H(1)$. If we can find a smooth path $H(g)$, $0 \le g \le 1$ that connect the two Hamiltonian $H(0)$ and $H(1)$ such that there is no phase transition along the path, then the two quantum ground states $|\Phi(0)\rangle$ and $|\Phi(1)\rangle$ belong to the same phase. We note that "connected by a smooth path" define an equivalence relation between quantum states. A quantum phase is an equivalence class of such equivalence relation. Such an equivalence class is called an universality class.

If $|\Phi(0)\rangle$ is the ground state of $H(0)$ and in the limit of infinite system size all excitations above $|\Phi(0)\rangle$ have a gap, then for small enough g, we believe that the systems described by $H(g)$ are also gapped.[34] In this case, we can show that, the ground state of $H(g)$, $|\Phi(g)\rangle$, is in the same phase as $|\Phi(0)\rangle$, for small enough g, i.e., the average $\langle O\rangle(g)$ is a smooth function of g near $g=0$ for any local operator O.[35] After scaling g to 1, we find that: *if the energy gap for $H(g)$ is finite for all g in the segment [0,1], then there is no phase transition along the path g*.

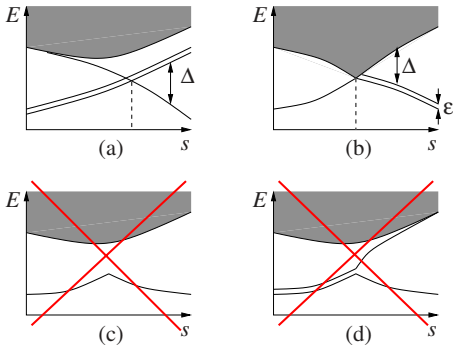

FIG. 1. (Color online) Energy spectrum of a gapped system as a function of a parameter s in the Hamiltonian. [(a) and (b)] For gapped system, a quantum phase transition can happen only when energy gap closes. (a) describes a first-order quantum phase transition (caused by level crossing). (b) describes a continuous quantum phase transition which has a continuum of gapless excitations at the transition point. (c) and (d) cannot happen for generic states. A gapped system may have ground-state degeneracy, where the energy splitting between the ground states vanishes when system size $L \to \infty$: $\lim_{L\to\infty} \epsilon = 0$. The energy gap Δ between ground and excited states on the other hand remains finite as $L \to \infty$.

In other words, for gapped system, a quantum phase transition can happen only when energy gap closes[35] (see Fig. 1).[36] Here, we would like to assume that the reverse is also true: a closing of the energy gap for a gapped state always induces a phase transition. Or more precisely *if two gapped states $|\Phi(0)\rangle$ and $|\Phi(1)\rangle$ are in the same phase, then we can always find a family of Hamiltonian $H(g)$, such that the energy gap for $H(g)$ are finite for all g in the segment [0,1], and $|\Phi(0)\rangle$ and $|\Phi(1)\rangle$ are ground states of $H(0)$ and $H(1)$, respectively.*

The above two statements imply that two gapped quantum states are in the same phase $|\Phi(0)\rangle \sim |\Phi(1)\rangle$ if and only if they can be connected by an adiabatic evolution that does not close the energy gap.

Given two states, $|\Phi(0)\rangle$ and $|\Phi(1)\rangle$, determining the existence of such a gapped adiabatic connection can be hard. We would like to have a more operationally practical equivalence relation between states in the same phase. Here we would like to show that *two gapped states* $|\Phi(0)\rangle$ and $|\Phi(1)\rangle$ are in the same phase, if and only if they are related by a local unitary (LU) evolution. We define a LU evolution as a unitary operation generated by time evolution of a local Hamiltonian for a finite time. That is,

$$|\Phi(1)\rangle \sim |\Phi(0)\rangle \quad \text{iff} \quad |\Phi(1)\rangle = \mathcal{T}\left[e^{-i\int_0^1 dg \tilde{H}(g)}\right]|\Phi(0)\rangle, \quad (1)$$

where $\mathcal{T}$ is the path-ordering operator and $\tilde{H}(g)=\Sigma_i O_i(g)$ is a sum of local Hermitian operators. Note that $\tilde{H}(g)$ is in general different from the adiabatic path $H(g)$ that connects the two states.

First, assume that two states $|\Phi(0)\rangle$ and $|\Phi(1)\rangle$ are in the same phase, therefore we can find a gapped adiabatic path $H(g)$ between the states. The existence of a gap prevents the system to be excited to higher energy levels and leads to a local unitary evolution, the quasiadiabatic continuation as defined in Ref. 35, that maps from one state to the other. That is,

$$|\Phi(1)\rangle = U|\Phi(0)\rangle, \quad U = \mathcal{T}\left[e^{-i\int_0^1 dg\tilde{H}(g)}\right]. \tag{2}$$

The exact form of $\tilde{H}(g)$ is given in Refs. 34 and 35 and will be discussed in more detail in the Appendix.

On the other hand, the reverse is also true: if two gapped states $|\Phi(0)\rangle$ and $|\Phi(1)\rangle$ are related by a local unitary evolution, then they are in the same phase. Since $|\Phi(0)\rangle$ and $|\Phi(1)\rangle$ are related by a local unitary evolution, we have $|\Phi(1)\rangle = \mathcal{T}[e^{-i\int_0^1 dg\tilde{H}(g)}]|\Phi(0)\rangle$. Let us introduce

$$|\Phi(s)\rangle = U(s)|\Phi(0)\rangle, \quad U(s) = \mathcal{T}\left[e^{-i\int_0^s dg\tilde{H}(g)}\right]. \tag{3}$$

Assume $|\Phi(0)\rangle$ is a ground state of $H(0)$, then $|\Phi(s)\rangle$ is a ground state of $H(s)=U(s)HU^\dagger(s)$. If $H(s)$ remains local and gapped for all $s\in[0,1]$, then we have found an adiabatic connection between $|\Phi(0)\rangle$ and $|\Phi(1)\rangle$.

First, let us show that $H(s)$ is a local Hamiltonian. Since H is a local Hamiltonian, it has a form $H=\Sigma_i O_i$, where O_i only acts on a cluster whose size is ξ. ξ is called the range of interaction of H. We see that $H(s)$ has a form $H(s)=\Sigma_i O_i(s)$, where $O_i(s)=U(s)O_iU^\dagger(s)$. To show that $O_i(s)$ only acts on a cluster of a finite size, we note that for a local system described by $\tilde{H}(g)$, the propagation velocities of its excitations have a maximum value $v_{\max}$. Since $O_i(s)$ can be viewed as the time evolution of O_i by $\tilde{H}(t)$ from $t=0$ to $t=s$, we find that $O_i(s)$ only acts on a cluster of size $\xi+\tilde{\xi}+sv_{\max}$,[35,37] where $\tilde{\xi}$ is the range of interaction of $\tilde{H}$. Thus $H(s)$ are indeed local Hamiltonian.

If H has a finite energy gap, then $H(s)$ also have a finite energy gap for any s. As s goes for 0 to 1, the ground state of the local Hamiltonians, $H(s)$, goes from $|\Phi(0)\rangle$ to $|\Phi(1)\rangle$. Thus the two states $|\Phi(0)\rangle$ and $|\Phi(1)\rangle$ belong to the same phase. This completes our argument that states related by a local unitary evolution belong to the same phase.

The finiteness of the evolution time is very important in the above discussion. Here "finite" means the evolution time does not grow with system size and in the thermodynamic limit, phases remain separate under such evolutions, as proven in Ref. 38. On the other hand, if the system size under consideration is finite, there is a critical time limit above which phase separation could be destroyed. The time limit depends on the propagation speed of interactions in the Hamiltonian. This is the case in Ref. 39, where topological order as measured by topological entropy and fidelity was found to decay under certain local Hamiltonian evolution (a quantum quench). However this result does not contradict our statement. As the calculation is done for a particular system size, the critical time limit could be below or above the time period they studied. If the calculation could be done for larger and larger system sizes for a fixed amount of time, we expect that topological order should emerge as stable against local quenches.

Thus through the above discussion, we show that *two gapped ground states,*[40] $|\Phi(0)\rangle$ *and* $|\Phi(1)\rangle$ *, belong to the same phase if and only if they are related by a local unitary evolution [Eq. (1)].* A more detailed and more rigorous discussion of this equivalence relation is given in the Appendix, where exact bounds on locality and transformation error is given.

The relation [Eq. (1)] defines an equivalence relation between $|\Phi(0)\rangle$ and $|\Phi(1)\rangle$. The equivalence classes of such an equivalence relation represent different quantum phases. So the above result implies that the equivalence classes of the LU evolutions are the universality classes of quantum phases for gapped states.

IV. TOPOLOGICAL ORDER IS A PATTERN OF LONG-RANGE ENTANGLEMENT

Using the LU evolution, we can obtain a more precise description (or definition) of short-range entanglement: *a state has only short-range entanglement if and only if it can be transformed into an unentangled state (i.e., a direct-product state) through a local unitary evolution.*

If a state cannot be transformed into an unentangled state through a LU evolution, then the state has long-range entanglement (LRE). We also see that *all states with short-range entanglement can transform into each other through local unitary evolutions.*

Thus all states with short-range entanglement belong to the same phase. The local unitary evolutions we consider here do not have any symmetry. If we require certain symmetry of the local unitary evolutions, states with short-range entanglement may belong to different symmetry breaking phases, which will be discussed in Sec. VI.

Since a direct-product state is a state with trivial topological order, we see that a state with a short-range entanglement also has a trivial topological order. This leads us to conclude that a nontrivial topological order is related to long-range entanglement. Since two gapped states related by a LU evolution belong to the same phase, thus two gapped states related by a local unitary evolution have the same topological order. In other words, *topological order describes the equivalent classes defined by local unitary evolutions.*

Or more pictorially, topological order is a pattern of long-range entanglement. In Ref. 38, it was shown that the "topologically nontrivial" ground states, such as the toric code,[27] cannot be changed into a "topologically trivial" state such as a product state by any unitary locality-preserving operator. In other words, those topologically nontrivial ground states have long-range entanglement.

V. LU EVOLUTIONS AND QUANTUM CIRCUITS

The LU evolutions introduced here is closely related to *quantum circuits with finite depth*. To define quantum circuits, let us introduce piecewise local unitary operators. A piecewise local unitary operator has a form $U_{pwl}=\Pi_i U_i$,

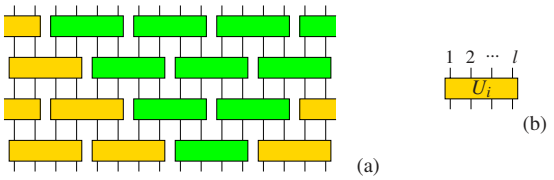

FIG. 2. (Color online) (a) A graphic representation of a quantum circuit, which is formed by (b) unitary operations on patches of finite size l. The dark shading represents a causal structure.

where $\{U_i\}$ is a set of unitary operators that act on nonoverlapping regions. The size of each region is less than some finite number l. The unitary operator U_{pwl} defined in this way is called a piecewise local unitary operator with range l. A quantum circuit with depth M is given by the product of M piecewise local unitary operators (see Fig. 2): $U^M_{circ}=U^{(1)}_{pwl}U^{(2)}_{pwl}\cdots U^{(M)}_{pwl}$. In quantum information theory, it is known that finite time unitary evolution with local Hamiltonian (LU evolution defined before) can be simulated with constant depth quantum circuit and vice versa. Therefore, the equivalence relation [Eq. (1)] can be equivalently stated in terms of constant depth quantum circuits,

$$|\Phi(1)\rangle \sim |\Phi(0)\rangle \quad \text{iff} \quad |\Phi(1)\rangle = U^M_{circ}|\Phi(0)\rangle, \tag{4}$$

where M is a constant independent of system size. Because of their equivalence, we will use the term "local unitary transformation" to refer to both local unitary evolution and constant depth quantum circuit in general.

The LU transformation defined through LU evolution [Eq. (1)] is more general. It can be easily generalized to study topological orders and quantum phases with symmetries (see Sec. VI).[30,41] The quantum circuit has a more clear and simple causal structure. However, the quantum circuit approach breaks the translation symmetry. So it is more suitable for studying quantum phases that do not have translation symmetry.

In fact, people have been using quantum circuits to classify many-body quantum states which correspond to quantum phases of matter. In Ref. 42, the local unitary transformations described by quantum circuits was used to define a renormalization-group (RG) transformations for states and establish an equivalence relation in which states are equivalent if they are connected by a local unitary transformation. Such an approach was used to classify one-dimensional matrix product states. In Ref. 43, the local unitary transformations with disentanglers was used to perform a renormalization-group transformations for states, which give rise to the multiscale entanglement renormalization ansatz (MERA) in one and higher dimensions. The disentanglers and the isometries in MERA can be used to study quantum phases and quantum phase transitions in one and higher dimensions. For a class of exactly solvable Hamiltonians which come from the stabilizer codes in quantum computation, topological order has also been classified using local unitary circuits.[44] Later in this paper, we will use the quantum circuit description of LU transformations to classify two-dimensional (2D) topological orders through classifying the fixed-point LU transformations.

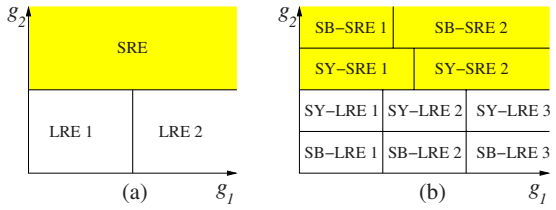

FIG. 3. (Color online) (a) The possible phases for a Hamiltonian $H(g_1,g_2)$ without any symmetry. (b) The possible phases for a Hamiltonian $H_{\text{symm}}(g_1,g_2)$ with some symmetries. The shaded regions in (a) and (b) represent the phases with short-range entanglement (i.e., those ground states can be transformed into a direct product state via a generic LU transformations that do not have any symmetry).

VI. SYMMETRY-BREAKING ORDERS AND SYMMETRY PROTECTED TOPOLOGICAL ORDERS

In the above discussions, we have defined phases without any symmetry consideration. The $\tilde{H}(g)$ or U_{pwl} in the LU transformation does not need to have any symmetry and can be sum/product of any local operators. In this case, two Hamiltonians with an adiabatic connection are in the same phase even if they may have different symmetries. Also, all states with short-range entanglement belong to the same phase (under the LU transformations that do not have any symmetry).

On the other hand, we can consider only Hamiltonians H with certain symmetries and define phases as the equivalent classes of symmetric local unitary transformations,

$$|\Psi\rangle \sim \mathcal{T}\left(e^{-i\int_0^1 dg\tilde{H}(g)}\right)|\Psi\rangle \quad \text{or} \quad |\Psi\rangle \sim U^M_{circ}|\Psi\rangle,$$

where $\tilde{H}(g)$ or U^M_{circ} has the same symmetries as H. We note that the symmetric local unitary transformation in the form $\mathcal{T}(e^{-i\int_0^1 dg\tilde{H}(g)})$ always connect to the identity transformation continuously. This may not be the case for the transformation in the form U^M_{circ}. To rule out that possibility, we define symmetric local unitary transformations as those that connect to the identity transformation continuously.

The equivalent classes of the symmetric LU transformations have very different structures compared to those of LU transformations without symmetry. Each equivalent class of the symmetric LU transformations is smaller and there are more kinds of classes, in general.

Figure 3 compares the structure of phases for a system without any symmetry and a system with some symmetry in more detail. For a system without any symmetry, all the SRE states (i.e., those ground states can be transformed into a direct product state via a generic LU transformations that do not have any symmetry) are in the same phase [SRE in Fig. 3(a)]. On the other hand, LRE can have many different patterns that give rise to different topological phases [LRE 1 and LRE 2 in Fig. 3(a)]. The different topological orders usually give rise to quasiparticles with different fractional statistics and fractional charges.

For a system with some symmetries, the phase structure can be much more complicated. The short-range-entangled states no longer belong to the same phase since the equiva-

lence relation is described by more special symmetric LU transformations: (A) states with short-range entanglement belong to different equivalent classes of the symmetric LU transformations if they have different broken symmetries. They correspond to the SB short-range-entanglement phases SB-SRE 1 and SB-SRE 2 in Fig. 3(b). They are Landau's symmetry-breaking states.

(B) States with short-range entanglement can belong to different equivalent classes of the symmetric LU transformations even if they do not break any symmetry of the system. (In this case, they have the same symmetry.) They correspond to the symmetric (SY) short-range-entangled phases SY-SRE 1 and SY-SRE 2 in Fig. 3(b). We say those states have symmetry protected topological orders. Haldane phase[45] and $S_z=0$ phase of spin-1 chain are examples of states with the same symmetry which belong to two different equivalent classes of symmetric LU transformations (with parity symmetry).[41,46] Band and topological insulators[47–52] are other examples of states that have the same symmetry and at the same time belong to two different equivalent classes of symmetric LU transformations (with time reversal symmetry). Also, for a system with some symmetries, the long-range-entangled states are divided into more classes (more phases).

(C) Symmetry-breaking and long-range entanglements can appear together in a state, such as SB-LRE 1, SB-LRE 2, etc., in Fig. 3(b). The topological superconducting states are examples of such phases.[53,54]

(D) Long-range-entangled states that do not break any symmetry can also belong to different phases such as the symmetric long-range-entanglement phases SY-LRE 1, SY-LRE 2, etc., in Fig. 3(b). The many different $\mathbb{Z}_2$ symmetric spin liquids with spin rotation, translation, and time-reversal symmetries are examples of those phases.[30,55,56] Some time-reversal symmetric topological orders were also called topological Mott insulators or fractionalized topological insulators.[57–62]

VII. LOCAL UNITARY TRANSFORMATION AND WAVE FUNCTION RENORMALIZATION

After defining topological order as the equivalent classes of many-body wave functions under LU transformations, we like to ask: how to describe (or label) the different equivalent classes (i.e., the different topological orders or patterns of long-range entanglement)?

One simple way to do so is to use the full wave function which completely describe the different topological orders. But the full wave functions contain a lot of nonuniversal short-range entanglement. As a result, such a labeling scheme is a very inefficient many-to-one labeling scheme of topological orders. To find a more efficient or even one-to-one labeling scheme, we need to remove the nonuniversal short-range entanglement.

As the first application of the notion of LU transformation, we would like to describe a wave function renormalization-group flow introduced in Refs. 43 and 63. The wave function renormalization can remove the short-range entanglement and simplify the wave function. In Ref. 63, the wave function renormalization for string-net states is generated by the following two basic moves:

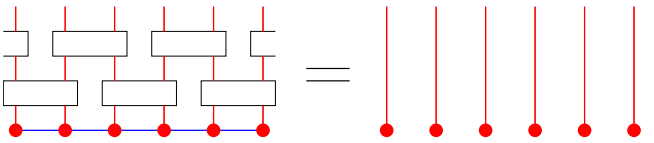

FIG. 4. (Color online) A finite depth quantum circuit can transform a state $|\Phi\rangle$ into a direct-product state, if and only if the state $|\Phi\rangle$ has no long-range quantum entanglement. Here, a dot represents a site with physical degrees of freedom. A vertical line carries an index that label the different physical states on a site. The presence of horizontal lines between dots represents quantum entanglement.

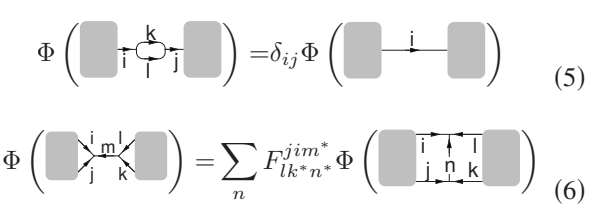

(Note that the definition of the F-tensor in Ref. 63 is slightly different from the definition in this paper.) The two basic moves can generate a generic wave function renormalization which can reduce the string-net wave functions to very simple forms.[17,63] Later in Ref. 43, the wave function renormalization for generic states was discussed in a more general setting, and was called MERA. The two basic string-net moves [Eqs. (5) and (6)] correspond to the isometry and the disentangler in MERA, respectively. In the MERA approach, the isometries and the disentanglers are applied in a layered fashion while in the string-net approach, the two basic moves can be applied arbitrarily. In this section, we will follow the MERA setup to describe the wave function renormalization. Later in this paper, we will follow the string-net setup to study the fixed-point wave functions.

Note that we can use a LU transformation U to transform some degrees of freedom in a state into direct product (see Figs. 4 and 5). We then remove those degrees of freedom in the form of direct product. Such a procedure does not change the topological order. The reverse process of adding degrees of freedom in the form of direct product also does not change the topological order. We call the local transformation in Fig. 5 that changes the degrees of freedom a generalized local

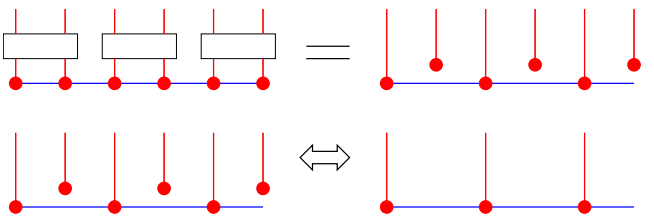

FIG. 5. (Color online) A piecewise local unitary transformation can transform some degrees of freedom in a state Φ into a direct product. Removing/adding the degrees of freedom in the form of direct product defines an additional equivalence relation that defines the topological order (or classes of long-range entanglement).

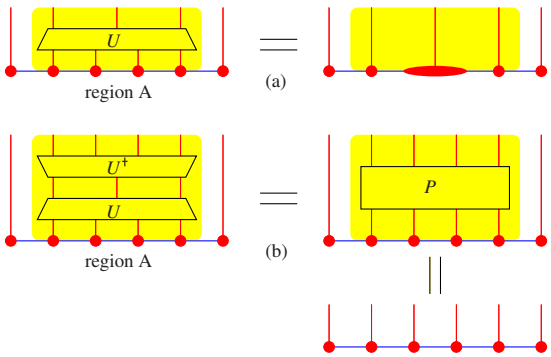

FIG. 6. (Color online) (a) A gLU transformation U acts in region A of a state $|\Phi\rangle$, which reduces the degree of freedom in region A to those contained only in the support space of $|\Phi\rangle$ in region A. (b) $U^\dagger U = P$ is a projector that does not change the state $|\Phi\rangle$.

unitary (gLU) transformation. It is clear that a generalized local unitary transformation inside a region A does not change the reduced density matrix ρ_A for the region A. This is the reason why we say that (generalized) local unitary transformations cannot change long-range entanglement and topological order. Similarly, the addition or removal of decoupled degrees of freedom to or from the Hamiltonian, $H \leftrightarrow H \otimes H_{dp}$, will not change the phase of the Hamiltonian (i.e., the ground states of H and $H \otimes H_{dp}$ are in the same phase), if those degrees of freedom form a direct product state (i.e., the ground state of H_{dp} is a direct product state).

Let us define the gLU transformation U more carefully and in a more general setting. Consider a state $|\Phi\rangle$. Let ρ_A be the reduced density matrix of $|\Phi\rangle$ in region A. ρ_A may act in a subspace of the total Hilbert space V_A in region A, which is called the support space V_A^{sp} of region A. The dimension D_A^{sp} of V_A^{sp} is called support dimension of region A. Now the Hilbert space V_A in region A can be written as $V_A = V_A^{sp} \oplus \bar{V}_A^{sp}$. Let $|\tilde{\psi}_i\rangle$, $i=1,\ldots,D_A^{sp}$ be a basis of this support space V_A^{sp}, $|\tilde{\psi}_i\rangle$, $i=D_A^{sp}+1,\ldots,D_A$ be a basis of $\bar{V}_A^{sp}$, where D_A is the dimension of V_A, and $|\psi_i\rangle$, $i=1,\ldots,D_A$ be a basis of V_A. We can introduce a LU transformation U^{full} which rotates the basis $|\psi_i\rangle$ to $|\tilde{\psi}_i\rangle$. We note that in the new basis, the wave function only has nonzero amplitudes on the first D_A^{sp} basis vectors. Thus, in the new basis $|\tilde{\psi}_i\rangle$, we can reduce the range of the label i from $[1, D_A]$ to $[1, D_A^{sp}]$ without losing any information. This motivates us to introduce the gLU transformation as a rotation from $|\psi_i\rangle$, $i=1,\ldots,D_A$ to $|\tilde{\psi}_i\rangle$, $i=1,\ldots,D_A^{sp}$. The rectangular matrix U is given by $U_{ij} = \langle\tilde{\psi}_i|\psi_j\rangle$. We also regard the inverse of $U, U^\dagger$, as a gLU transformation. A LU transformation is viewed as a special case of gLU transformation where the degrees of freedom are not changed. Clearly $U^\dagger U = P$ and $UU^\dagger = P'$ are two projectors. The action of P does not change the state $|\Phi\rangle$ [see Fig. 6(b)].

We note that despite the reduction in the degrees of freedom, a gLU transformation defines an equivalent relation. Two states related by a gLU transformation belong to the same phase. The renormalization flow induced by the gLU transformations always flows within the same phase.

VIII. WAVE FUNCTION RENORMALIZATION AND A CLASSIFICATION OF TOPOLOGICAL ORDER

As an application of the wave function renormalization, in this section, we will study the structure of fixed-point wave functions under the wave function renormalization, which will lead to a classification of topological order (without any symmetry).

We note that as wave functions flow to a fixed point, the gLU transformations in each step of the renormalization also flow to a fixed point. So instead of studying fixed-point wave functions, here, we will study the fixed-point gLU transformations. For this purpose, we need to fix the renormalization scheme. In the following, we will discuss a renormalization scheme motivated by the string-net wave function.[63] After we specify a proper wave function renormalization scheme, then the fixed-point wave function is simply the wave function whose "form" does not change under the wave function renormalization.

Since those fixed-point gLU transformations do not change the fixed-point wave function, their actions on the fixed-point wave function do not depend on the order of the actions. This allows us to obtain many conditions that gLU transformations must satisfy. From those conditions, we can determine the forms of allowed fixed-point gLU transformations. This leads to a general description and a classification of topological orders and their corresponding fixed-point wave functions.

The renormalization scheme that we will discuss was first used in Ref. 63 to characterize the scale invariant string-net wave function. It is also used in Ref. 17 to simplify the string-net state in a region, which allows us to calculate the entanglement entropy of the string-net state exactly. A similar approach was used in Ref. 64 to show quantum-double/string-net wave function to be a fixed-point wave function and its connection to 2D MERA.[43] In the following, we will generalize those discussions by not starting with string-net wave functions. We just try to construct local unitary transformations at a fixed point. We will see that the fixed-point conditions on the gLU transformations lead to a mathematical structure that is similar to the tensor category theory—the mathematical framework behind the string-net states.

A. Quantum states on a graph

Since the wave function renormalization may change the lattice structure, we will consider quantum states defined on a generic trivalence graph G: each edge has $N+1$ states, labeled by $i=0,\ldots,N$ (see Fig. 7). We assume that the index i on the edge admits an one-to-one mapping $*$: $i \to i^*$ that satisfies $(i^*)^* = i$. As a result, the edges of the graph are oriented. The mapping $i \to i^*$ corresponds to the reverse of the orientation of the edge (see Fig. 8). Each vertex also has physical states, labeled by $\alpha=1,\ldots,N_v$ (see Fig. 7).

Each labeled graph (see Fig. 7) corresponds to a state and all the labeled graphs form an orthonormal basis. Our fixed-point state is a superposition of those basis states:

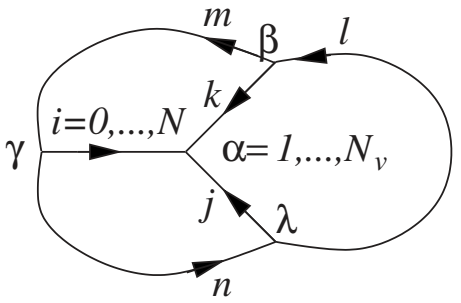

FIG. 7. A quantum state on a graph G. There are $N+1$ states on each edge which are labeled by $l=0,\ldots,N$. There are N_v states on each vertex which are labeled by $\alpha=1,\ldots,N_v$.

$$|\Phi_{\text{fix}}\rangle = \sum_{\text{all conf.}} \Phi_{\text{fix}} \left(\quad \right) \left| \quad \right\rangle .$$

Here we will make an important assumption about the fixed-point wave function. We will assume that the fixed-point wave function is "topological:" two labeled graphs have the same amplitude if the two labeled graphs can be deformed into each other continuously on the plane without the vertices crossing the links. For example,

$$\psi_{\text{fix}} \left(\quad \right) = \psi_{\text{fix}} \left(\quad \right)$$

Due to such an assumption, the topological orders studied in this paper may not be most general.

We also assume that all the fixed-point states on each different graphs to have the same form. This assumption is motivated by the fact that during wave function renormalization, we transform a state on one graph to a state on a different graph. The "fixed point" means that the wave functions on those different graphs are all determined by the same collection of the rules, which defines the meaning of having the same form. However, the wave function for a given graph can have different total phases if the wave function is calculated by applying the rules in different orders. Those rules are noting but the fixed-point gLU transformations.

B. Structure of entanglement in a fixed-point wave function

Before describing the wave function renormalization, let us examine the structure of entanglement of a fixed-point wave function. First, let us consider a fixed-point wave function Φ_{fix} on a graph. We examine the wave function on a patch of the graph, for example,

FIG. 8. The mapping $i \to i^*$ corresponds to the reverse of the orientation of the edge.

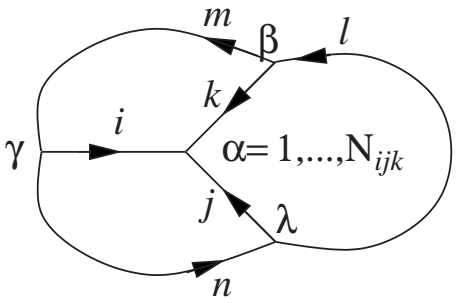

FIG. 9. A quantum state on a graph G. If the three edges of a vertex are in the states i, j, and k, respectively, then the vertex has N_{ijk} states, labeled by $\alpha=1,\ldots,N_{ijk}$. Note the orientation of the edges are point toward to vertex. Also note that $i \to j \to k$ runs anticlockwise.

The fixed-point wave function

$$\Phi_{\text{fix}} \left(\quad \right)$$

(only the relevant part of the graph is drawn) can be viewed as a function of α, β, m:

$$\psi_{ijkl,\Gamma}(\alpha,\beta,m) = \Phi_{\text{fix}} \left(\quad \right)$$

if we fix i,j,k,l and the indices on other part of the graph. (Here the indices on other part of the graph is summarized by Γ.) As we vary the indices Γ on other part of graph (still keeping i, j, k, and l fixed), the wave function of α,β,m, $\psi_{ijkl,\Gamma}(\alpha,\beta,m)$, may change. All those $\psi_{ijkl,\Gamma}(\alpha,\beta,m)$ form a linear space of dimension D_{ijkl^*}. D_{ijkl} is an important concept that will appear later. We note that the two vertices α and β and the link m form a region surrounded by the links i,j,k,l. So we will call the dimension-D_{ijkl^*} space the support space V_{ijkl^*} and D_{ijkl^*} the support dimension for the state Φ_{fix} on the region surrounded by the fixed boundary state i,j,k,l.

Similarly, we can define D_{ijk} as the support dimension of the

$$\Phi_{\text{fix}} \left(\quad \right)$$

on a region bounded by links i,j,k. Since the region contains only a single vertex α with N_v physics states, we have $D_{ijk} \leq N_v$. We can use a local unitary transformation on the vertex to reduce the range of α to $1,\ldots,N_{ijk}$, where $N_{ijk}=D_{ijk}$. In the rest of this paper, we will implement such a reduction. So, the number of physical states on a vertex depend on the physical states of the edges that connect to the vertex. If the three edges of a vertex are in the states i, j, and k, respectively, then the vertex has N_{ijk} states, labeled by $\alpha=1,\ldots,N_{ijk}$ (see Fig. 9). Here we assume that

$$N_{ijk} = N_{jki}. \tag{7}$$

We note that in the fixed-point wave function

$$\Phi_{\text{fix}}\left(\right),$$

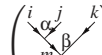

the number of choices of α,β,m is $N_{ijkl^*}=\Sigma_{m=0}^{N}N_{jim^*}N_{kml^*}$. Thus the support dimension D_{ijkl^*} satisfies $D_{ijkl^*}\leq N_{ijkl^*}$. Here we will make an important assumption—the saturation assumption: *the fixed-point wave function saturate the inequality*,

$$D_{ijkl^*}=N_{ijkl^*}\equiv\sum_{m=0}^{N}N_{jim^*}N_{kml^*}. \tag{8}$$

We will see that the entanglement structure described by such a saturation assumption is invariant under the wave function renormalization.

C. First type of wave function renormalization

Our wave function renormalization scheme contains two types of renormalization. The first type of renormalization does not change the degrees of freedom and corresponds to a local unitary transformation. It corresponds to locally deform the graph

to

(The parts that are not drawn are the same.) The fixed-point wave function on the new graph is given by

$$\Phi_{\text{fix}}\left(\right).$$

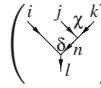

Again, such a wave function can be viewed as a function of χ,δ,n:

$$\tilde{\psi}_{ijkl,\Gamma}(\chi,\delta,n)=\Phi_{\text{fix}}\left(\right)$$

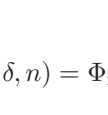

if we fix i,j,k,l and the indices on other part of the graph. The support dimension of the state

$$\Phi_{\text{fix}}\left(\right)$$

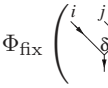

on the region surrounded by i,j,k,l is $\tilde{D}_{ijkl^*}$. Again $\tilde{D}_{ijkl^*}\leq\tilde{N}_{ijkl^*}$, where $\tilde{N}_{ijkl^*}\equiv\Sigma_{n=0}^{N}N_{kjn^*}N_{l^*ni}$ is number of choices of χ,δ,n. The saturation assumption implies that $\tilde{N}_{ijkl^*}=\tilde{D}_{ijkl^*}$.

The two fixed-point wave functions

$$\Phi_{\text{fix}}\left(\right)$$

and

$$\Phi_{\text{fix}}\left(\right)$$

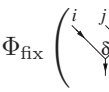

are related via a local unitary transformation. Thus $D_{ijkl^*}=\tilde{D}_{ijkl^*}$, which implies

$$\sum_{m=0}^{N}N_{jim^*}N_{kml^*}=\sum_{n=0}^{N}N_{kjn^*}N_{l^*ni}. \tag{9}$$

We express such an unitary transformation as

$$\psi_{ijkl,\Gamma}(\alpha,\beta,m)\simeq\sum_{n=0}^{N}\sum_{\chi=1}^{N_{kjn^*}}\sum_{\delta=1}^{N_{nil^*}}F_{kln,\chi\delta}^{ijm,\alpha\beta}\tilde{\psi}_{ijkl,\Gamma}(\chi,\delta,n) \tag{10}$$

or graphically as

$$\Phi_{\text{fix}}\left(\right)\simeq\sum_{=0}^{N}\sum_{=1}^{N_{kjn^*}}\sum_{\delta=1}^{N_{nil^*}}F_{kln,\chi\delta}^{ijm,\alpha\beta}\Phi_{\text{fix}}\left(\right). \tag{11}$$

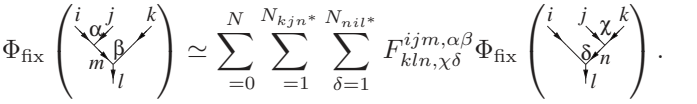

where $\simeq$ means equal up to a constant phase factor. (Note that the total phase of the wave function is unphysical.) We will call such a wave function renormalization step a F-move.

We would like to remark that Eq. (11) relates two wave functions on two graphs G_1 and G_2 which only differ by a local reconnection. We can choose the phase of $F_{kln,\chi\delta}^{ijm,\alpha\beta}$ to make $\simeq$ into =:

$$\Phi_{\text{fix}}\left(\right)=\sum_{n=0}^{N}\sum_{\chi=1}^{N_{kjn^*}}\sum_{\delta=1}^{N_{nil^*}}F_{kln,\chi\delta}^{ijm,\alpha\beta}\Phi_{\text{fix}}\left(\right).$$

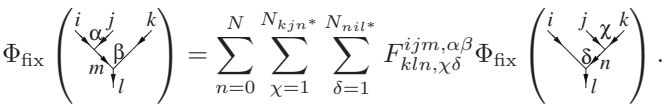

But such choice of phase only works for a particular pair of graphs G_1 and G_2. To use $F_{kln,\chi\delta}^{ijm,\alpha\beta}$ to relate all pair of states that only differ by a local reconnection, in general, we may have a phase ambiguity, with the value of phase depend on

the pair of graphs. So Eq. (11) can only be a relation up to a total phase factor.

For fixed i, j, k, and l, the matrix F^{ij}_{kl} with matrix elements $(F^{ij}_{kl})^{m,\alpha\beta}_{n,\chi\delta}=F^{ijm,\alpha\beta}_{kln,\chi\delta}$ is a N_{ijkl^*} dimensional matrix [see Eq. (9)]. The mapping $\tilde{\psi}_{ijkl,\Gamma}(\chi,\delta,n)\to\psi_{ijkl,\Gamma}(\alpha,\beta,m)$ generated by the matrix F^{ij}_{kl} is unitary. Since, as we change Γ, $\tilde{\psi}_{ijkl,\Gamma}(\chi,\delta,n)$ and $\psi_{ijkl,\Gamma}(\alpha,\beta,m)$ span two N_{ijkl^*}-dimensional spaces. Thus F^{ij}_{kl} is a $N_{ijkl^*}\times N_{ijkl^*}$ unitary matrix

$$\sum_{n,\chi,\delta} F^{ijm',\alpha'\beta'}_{kln,\chi\delta}(F^{ijm,\alpha\beta}_{kln,\chi\delta})^*=\delta_{m\alpha\beta,m'\alpha'\beta'}, \tag{12}$$

where $\delta_{m\alpha\beta,m'\alpha'\beta'}=1$ when $m=m'$, $\alpha=\alpha'$, $\beta=\beta'$, and $\delta_{m\alpha\beta,m'\alpha'\beta'}=0$ otherwise.

We can deform

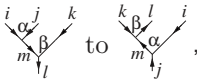

and

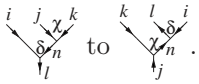

We see that

$$\Phi_{\text{fix}}\left(\begin{array}{c}\text{k β l i}\\ \text{α}\\ \text{m}\quad\text{j}\end{array}\right)\simeq\sum_{n=0}^{N}\sum_{\chi,\delta}F^{kl^*m^*,\beta\alpha}_{ij^*n^*,\delta\chi}\Phi_{\text{fix}}\left(\begin{array}{c}\text{k l i}\\ \text{χ δ}\\ \text{n}\\ \text{j}\end{array}\right). \tag{13}$$

Equations (11) and (13) relate the same pair of graphs, and thus

$$F^{ijm,\alpha\beta}_{kln,\chi\delta}\simeq F^{kl^*m^*,\beta\alpha}_{ij^*n^*,\delta\chi} \tag{14}$$

(where we have used the condition $N_{ijkl}=D_{ijkl}$.)

Using the relation [Eq. (12)], we can rewrite Eq. (11) as

$$\Phi_{\text{fix}}\left(\begin{array}{c}\text{i j χ k}\\ \text{δ}\\ \text{n}\\ \text{l}\end{array}\right)\simeq\sum_{m=0}^{N}\sum_{\alpha,\beta}(F^{ijm,\alpha\beta}_{kln,\chi\delta})^*\Phi_{\text{fix}}\left(\begin{array}{c}\text{i α j k}\\ \text{β}\\ \text{m}\quad\text{l}\end{array}\right). \tag{15}$$

We can also express

$$\Phi_{\text{fix}}\left(\begin{array}{c}\text{i j χ k}\\ \text{δ}\\ \text{n}\\ \text{l}\end{array}\right)$$

as

$$\Phi_{\text{fix}}\left(\begin{array}{c}\text{i j χ k}\\ \text{δ}\\ \text{n}\\ \text{l}\end{array}\right)\simeq\sum_{m=0}^{N}\sum_{\alpha,\beta}F^{jkn,\chi\delta}_{l^*i^*m^*,\beta\alpha}\Phi_{\text{fix}}\left(\begin{array}{c}\text{i α j k}\\ \text{β}\\ \text{m}\quad\text{l}\end{array}\right) \tag{16}$$

using the relabeled Eq. (11). So we have

$$(F^{ijm,\alpha\beta}_{kln,\chi\delta})^*\simeq F^{jkn,\chi\delta}_{l^*i^*m^*,\beta\alpha}. \tag{17}$$

Since the total phase of the wave function is unphysical, the total phase of $F^{ijm,\alpha\beta}_{kln,\chi\delta}$ can be chosen arbitrarily. We can choose the total phase of $F^{ijm,\alpha\beta}_{kln,\chi\delta}$ to make

$$(F^{ijm,\alpha\beta}_{kln,\chi\delta})^*=F^{jkn,\chi\delta}_{l^*i^*m^*,\beta\alpha}. \tag{18}$$

If we apply Eq. (18) twice, we reproduce Eq. (14). Thus Eq. (14) is not independent and can be dropped.

From the graphic representation [Eq. (11)], We note that

$$F^{ijm,\alpha\beta}_{kln,\chi\delta}=0$$

when

$$N_{jim^*}<1 \quad\text{or}\quad N_{kml^*}<1 \quad\text{or}\quad N_{kjn^*}<1 \quad\text{or}\quad N_{nil^*}<1. \tag{19}$$

When $N_{jim^*}<1$ or $N_{kml^*}<1$, the left-hand side of Eq. (11) is always zero. Thus $F^{ijm,\alpha\beta}_{kln,\chi\delta}=0$ when $N_{jim^*}<1$ or $N_{kml^*}<1$. When $N_{kjn^*}<1$ or $N_{nil^*}<1$, wave function on the right-hand side of Eq. (11) is always zero. So we can choose $F^{ijm,\alpha\beta}_{kln,\chi\delta}=0$ when $N_{kjn^*}<1$ or $N_{nil^*}<1$.

The F-move [Eq. (11)] maps the wave functions on two different graphs through a local unitary transformation. Since we can locally transform one graph to another graph through different paths, the F-move [Eq. (11)] must satisfy certain self-consistent condition. For example, the graph

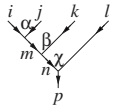

can be transformed to

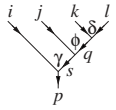

through two different paths; one contains two steps of local transformations and the other contains three steps of local transformations as described by Eq. (11). The two paths lead to the following relations between the wave functions:

$$\Phi_{\rm fix}\left(\begin{array}{c}\text{diagram}\end{array}\right) \simeq \sum_{q,\delta,\epsilon} F^{mkn,\beta\chi}_{lpq,\delta\epsilon}\Phi_{\rm fix}\left(\begin{array}{c}\text{diagram}\end{array}\right) \simeq \sum_{q,\delta,\epsilon;s,\phi,\gamma} F^{mkn,\beta\chi}_{lpq,\delta\epsilon}F^{ijm,\alpha\epsilon}_{qps,\phi\gamma}\Phi_{\rm fix}\left(\begin{array}{c}\text{diagram}\end{array}\right), \tag{20}$$

$$\Phi_{\rm fix}\left(\begin{array}{c}\text{diagram}\end{array}\right) \simeq \sum_{t,\eta,\varphi} F^{ijm,\alpha\beta}_{knt,\eta\varphi}\Phi_{\rm fix}\left(\begin{array}{c}\text{diagram}\end{array}\right) \simeq \sum_{t,\eta,\varphi;s,\kappa,\gamma} F^{ijm,\alpha\beta}_{knt,\eta\varphi}F^{itn,\varphi\chi}_{lps,\kappa\gamma}\Phi_{\rm fix}\left(\begin{array}{c}\text{diagram}\end{array}\right)$$

$$\simeq \sum_{t,\eta,\kappa;\varphi;s,\kappa,\gamma;q,\delta,\phi} F^{ijm,\alpha\beta}_{knt,\eta\varphi}F^{itn,\varphi\chi}_{lps,\kappa\gamma}F^{jkt,\eta\kappa}_{lsq,\delta\phi}\Phi_{\rm fix}\left(\begin{array}{c}\text{diagram}\end{array}\right). \tag{21}$$

The consistence of the above two relations leads a condition on the F tensor.

To obtain such a condition, let us fix i,j,k,l,p, and view

$$\Phi_{\rm fix}\left(\begin{array}{c}\text{diagram}\end{array}\right)$$

as a function of α,β,χ,m,n:

$$\psi(\alpha,\beta,\chi,m,n) = \Phi_{\rm fix}\left(\begin{array}{c}\text{diagram}\end{array}\right).$$

As we vary indices on other part of graph, we obtain different wave functions $\psi(\alpha,\beta,\chi,m,n)$ which form a dimension D_{ijklp^*} space. In other words, D_{ijklp^*} is the support dimension of the state $\Phi_{\rm fix}$ on the region α,β,χ,m,n with boundary state i,j,k,l,p fixed (see the discussion in Sec. VIII B). Since the number of choices of α,β,χ,m,n is $N_{ijklp^*}=\Sigma_{m,n}N_{jim^*}N_{kmn^*}N_{lnp^*}$, we have $D_{ijklp^*}\le N_{ijklp^*}$. Here we require a similar saturation condition as in Eq. (8),

$$N_{ijklp^*} = D_{ijklp^*}. \tag{22}$$

Similarly, the number of choices of δ,ϕ,γ,q,s in

$$\Phi_{\rm fix}\left(\begin{array}{c}\text{diagram}\end{array}\right)$$

is also N_{ijklp^*}. Here we again assume $\tilde{D}_{ijklp^*}=N_{ijklp^*}$, where $\tilde{D}_{ijklp^*}$ is the support dimension of

$$\Phi_{\rm fix}\left(\begin{array}{c}\text{diagram}\end{array}\right)$$

on the region bounded by i,j,k,l,p.

So the two relations [Eqs. (20) and (21)] can be viewed as two relations between a pair of vectors in the two D_{ijklp^*}-dimensional vector spaces. As we vary indices on other part of graph (still keeping i,j,k,l,p fixed), each vector in the pair can span the full D_{ijklp^*}-dimensional vector space. So the validity of the two relations [Eqs. (20) and (21)] implies that

$$\sum_{t}\sum_{\eta=1}^{N_{kjt^*}}\sum_{\varphi=1}^{N_{tin^*}}\sum_{\kappa=1}^{N_{lts^*}} F^{ijm,\alpha\beta}_{knt,\eta\varphi}F^{itn,\varphi\chi}_{lps,\kappa\gamma}F^{jkt,\eta\kappa}_{lsq,\delta\phi} = e^{i\theta_F}\sum_{\epsilon=1}^{N_{qmp^*}} F^{mkn,\beta\chi}_{lpq,\delta\epsilon}F^{ijm,\alpha\epsilon}_{qps,\phi\gamma}, \tag{23}$$

which is a generalization of the famous pentagon identity (due to the extra constant phase factor $e^{i\theta_F}$). We will call such a relation projective pentagon identity. The projective pentagon identity is a set of nonlinear equations satisfied by the rank-10 tensor $F^{ijm,\alpha\beta}_{kln,\chi\delta}$ and θ_F. The above consistency relation is equivalent to the requirement that the local unitary transformations described by Eq. (11) on different paths all commute with each other up to a total phase factor.

D. Second type of wave function renormalization

The second type of wave function renormalization does change the degrees of freedom and corresponds to a generalized local unitary transformation. One way to implement the second type renormalization is to reduce

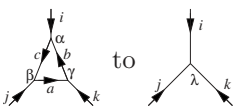

(the part of the graph that is not drawn is unchanged):

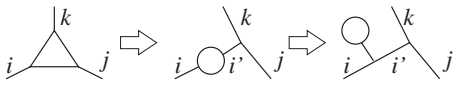

FIG. 10. A "triangle" graph can be transformed into a "tadpole" via two steps of the first type of wave function renormalization (i.e., two steps of local unitary transformations).

$$\Phi_{\text{fix}}\left(\quad\right) \simeq \sum_{\lambda=1}^{N_{ijk}} F_{ijk,\lambda}^{abc,\alpha\beta\gamma}\Phi_{\text{fix}}\left(\quad\right). \tag{24}$$

But we can define a simpler second type renormalization, by noting that

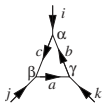

can be reduced to

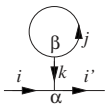

via the first type of renormalization steps (see Fig. 10), which are local unitary transformations. In the simplified second type renormalization, we want to reduce

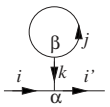

to

so that we still have a trivalence graph. This requires that the support dimension $D_{ii'^*}$ of the fixed-point wave function

$$\Phi_{\text{fix}}\left(\quad\right)$$

is given by

$$D_{ii'^*} = \delta_{ii'}. \tag{25}$$

This implies that

$$\Phi_{\text{fix}}\left(\quad\right) \simeq \delta_{ii'}\Phi_{\text{fix}}\left(\quad\right). \tag{26}$$

The simplified second type renormalization can now be written as (since $D_{ii^*}=1$)

$$\Phi_{\text{fix}}\left(\quad\right) \simeq P_i^{kj,\alpha\beta}\Phi_{\text{fix}}\left(\quad\right). \tag{27}$$

We will call such a wave function renormalization step a P-move.[64] Here $P_i^{kj,\alpha\beta}$ satisfies

$$\sum_{k,j}\sum_{\alpha=1}^{N_{kii^*}}\sum_{\beta=1}^{N_{j^*jk^*}} P_i^{kj,\alpha\beta}(P_i^{kj,\alpha\beta})^* = 1 \tag{28}$$

and

$$P_i^{kj,\alpha\beta} = 0, \quad \text{if } N_{kii^*} < 1 \quad \text{or} \quad N_{j^*jk^*} < 1. \tag{29}$$

The condition [Eq. (28)] ensures that the two wave functions on the two sides of Eq. (27) have the same normalization. We note that the number of choices for the four indices (j,k,α,β) in $P_i^{kj,\alpha\beta}$ must be equal or greater than 1,

$$D_i = \sum_{j,k} N_{ii^*k}N_{jk^*j^*} \geq 1. \tag{30}$$

Notice that

$$\Phi_{\text{fix}}\left(\quad\right) \simeq \sum_{m,\lambda,\gamma} F_{i^*i^*m^*,\lambda\gamma}^{jj^*k,\beta\alpha}\Phi_{\text{fix}}\left(\quad\right)$$

$$\simeq \sum_{m,\lambda,\gamma,l,\nu,\mu} F_{i^*i^*m^*,\lambda\gamma}^{jj^*k,\beta\alpha}F_{m^*i^*l,\nu\mu}^{i^*mj,\lambda\gamma}\Phi_{\text{fix}}\left(\quad\right) \tag{31}$$

Using Eq. (27) and its variation

$$\Phi_{\text{fix}}\left(\quad\right) \simeq P_{i^*}^{lm,\mu\nu}\Phi_{\text{fix}}\left(\quad\right). \tag{32}$$

we can rewrite Eq. (31) as

$$e^{i\theta_{P1}}P_i^{kj,\alpha\beta} = \sum_{m,\lambda,\gamma,l,\nu,\mu} F^{jj^*k,\beta\alpha}_{i^*i^*m^*,\lambda\gamma} F^{i^*mj,\lambda\gamma}_{m^*i^*l,\nu\mu} P_{i^*}^{lm,\mu\nu}, \quad (33)$$

which is a condition on $P_i^{kj,\alpha\beta}$.

More conditions on $F^{ijm,\alpha\beta}_{kln,\chi\delta}$ and $P_i^{kj,\alpha\beta}$ can be obtained by noticing that

$$\Phi_{\text{fix}}\left(\begin{array}{c} p \\ i \quad \eta \quad k \\ \alpha \quad j \\ m \quad \beta \\ l \end{array}\right) \simeq \sum_{n=0}^{N} \sum_{\chi,\delta} F^{ijm,\alpha\beta}_{kln,\chi\delta} \Phi_{\text{fix}}\left(\begin{array}{c} p \\ i \quad \eta \quad k \\ j \quad \chi \\ \delta \quad n \\ l \end{array}\right), \quad (34)$$

which implies that

$$P_i^{jp,\alpha\eta}\delta_{im}\Phi_{\text{fix}}\left(\begin{array}{c} i \quad \beta \quad k \\ l \end{array}\right) \simeq \sum_{n,\chi,\delta} F^{ijm,\alpha\beta}_{kln,\chi\delta} P_{k^*}^{jp,\chi\eta}\delta_{kn}\Phi_{\text{fix}}\left(\begin{array}{c} i \quad \delta \quad k \\ l \end{array}\right). \quad (35)$$

We find

$$e^{i\theta_{P2}}P_i^{jp,\alpha\eta}\delta_{im}\delta_{\beta\delta} = \sum_{\chi=1}^{N_{kjk^*}} F^{ijm,\alpha\beta}_{klk,\chi\delta} P_{k^*}^{jp,\chi\eta} \quad \text{for all } k,i,l \text{ satisfying } N_{kil^*} > 0. \quad (36)$$

E. Fixed-point wave functions from the fixed-point gLU transformations

In the last section, we discussed the conditions that a fixed-point gLU transformation $(F^{ijm,\alpha\beta}_{kln,\gamma\lambda}, P_i^{kj,\alpha\beta})$ must satisfy. After finding a fixed-point gLU transformation $(F^{ijm,\alpha\beta}_{kln,\gamma\lambda}, P_i^{kj,\alpha\beta})$, in this section, we are going to discuss how to calculate the corresponding fixed-point wave function Φ_{fix} from the solved fixed-point gLU transformation $(F^{ijm,\alpha\beta}_{kln,\gamma\lambda}, P_i^{kj,\alpha\beta})$.

First we note that, using the two types of wave function renormalization introduced above, we can reduce any graph to

So, once we know

$$\Phi_{\text{fix}}\left(\begin{array}{c} i \end{array}\right),$$

we can reconstruct the full fixed-point wave function Φ_{fix} on any connected graph.

Let us assume that

$$\Phi_{\text{fix}}\left(\begin{array}{c} i \end{array}\right) = A^i = A^{i^*} \quad (37)$$

Here A^i satisfy

$$A^i = A^{i^*}, \quad \sum_i A^i (A^i)^* = 1. \quad (38)$$

The condition $\Sigma_i A^i (A^i)^* = 1$ is simply the normalization condition of the wave function. The condition $A^i = A^{i^*}$ come from the fact that the graph

can be deformed into the graph

on a sphere.

To find the conditions that determine A^i, let us first consider the fixed-point wave function where the index on a link is i:

$$\Phi_{\text{fix}}(i,\Gamma) = \Phi_{\text{fix}}\left(\begin{array}{c} \Gamma \quad i \end{array}\right),$$

where Γ are indices on other part of graph. We note that the graph

can be deformed into the graph

on a sphere. Thus

$$\Phi_{\text{fix}}\left(\begin{array}{c} \Gamma \quad i \end{array}\right) = \Phi_{\text{fix}}\left(\begin{array}{c} i \\ \Gamma \end{array}\right).$$

Using the F-moves and the P-moves, we can reduce


to

:

$$\Phi_{\text{fix}}\left(\begin{array}{c} \Gamma \quad i \end{array}\right) = \Phi_{\text{fix}}\left(\begin{array}{c} i \\ \Gamma \end{array}\right) \simeq f(i,\Gamma)\Phi_{\text{fix}}\left(\begin{array}{c} i \end{array}\right) \quad (39)$$

We see that

$$\Phi_{\text{fix}}\left(\begin{array}{c} i \end{array}\right) = A^i \neq 0 \quad (40)$$

for all i. Otherwise, any wave function with i link will be zero.

To find more conditions on A^i, we note that

$$\Phi_{\text{fix}}\left(\begin{array}{c} \lambda \quad j \\ m \\ i \quad \gamma \end{array}\right) \simeq P_i^{mj,\gamma\lambda}\Phi_{\text{fix}}\left(\begin{array}{c} i \end{array}\right) = P_i^{mj,\gamma\lambda}A^i. \quad (41)$$

By rotating

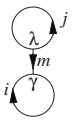

by 180°, we can show that $P_i^{mj,\gamma\lambda}A^i \simeq P_{j^*}^{m^*i^*,\lambda\gamma}A^j$ or

$$P_i^{mj,\gamma\lambda}A^i = e^{i\theta_{A1}}P_{j^*}^{m^*i^*,\lambda\gamma}A^j. \tag{42}$$

We also note that

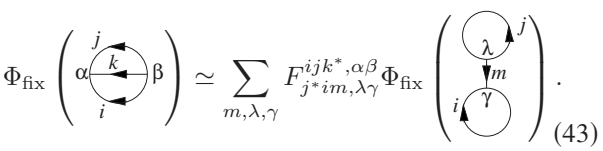

(43)

This allows us to show

$$\Phi^{\theta}_{ikj,\alpha\beta} = e^{i\theta'}\sum_{m,\lambda,\gamma} F^{ijk^*,\alpha\beta}_{j^*im,\lambda\gamma}P_i^{mj,\gamma\lambda}A^i, \tag{44}$$

where

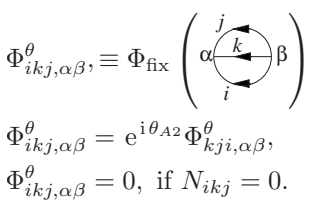

(45)

The condition $\Phi^{\theta}_{ikj,\alpha\beta} \simeq \Phi^{\theta}_{kji,\alpha\beta}$ comes from the fact that the graph

and the graph

can be deformed into each other on a sphere.

Also, for any given i,j,k,α that satisfy $N_{kji}>0$, the wave function

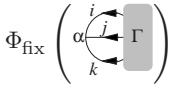

must be nonzero for some Γ, where Γ represents indices on other part of the graph. Then after some F-moves and P-moves, we can reduce

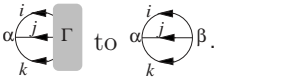

So, for any given i,j,k,α that satisfy $N_{kji}>0$,

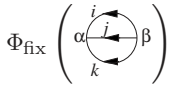

is nonzero for some β. Since such a statement is true for any choices of basis on the vertex α, we find that for any given i,j,k,α that satisfy $N_{kji}>0$ and for any nonzero vector v_α,

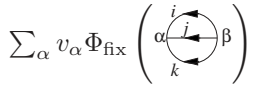

is nonzero for some β. This means that the matrix M_{kji} is invertible, where M_{kji} is a matrix whose elements are given by

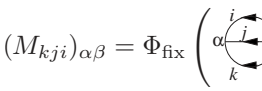

Let us define

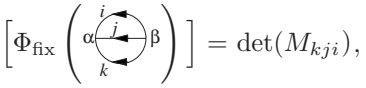

we find that

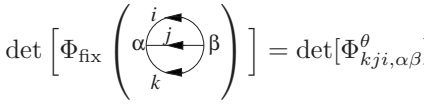

(46)

The above also implies that

$$N_{kji} = N_{i^*j^*k^*}. \tag{47}$$

The conditions [Eqs. (38), (42), (44), and (45)] allow us to determine A^i (and $\Phi^{\theta}_{ikj,\alpha\beta}$).

From Eq. (45), we see that relation

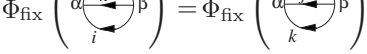

leads to some equations for $F^{ijm,\alpha\beta}_{kln,\gamma\lambda}$, $P_i^{kj,\alpha\beta}$, and A^i. More equations for $F^{ijm,\alpha\beta}_{kln,\gamma\lambda}$, $P_i^{kj,\alpha\beta}$, and A^i, can be obtained by using the relations

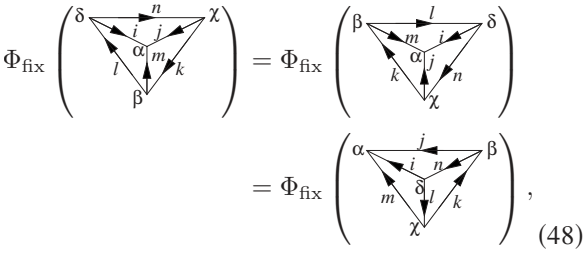

(48)

from the tetrahedron rotation symmetry[63,65] and

$$\Phi_{\text{fix}}\left(\right.$$
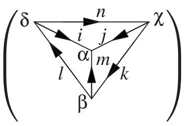

$$\left.\right) \simeq \sum_{\gamma\lambda} F^{ijm^*,\alpha\beta}_{kln,\gamma\lambda}\Phi_{\text{fix}}\left(\right.$$
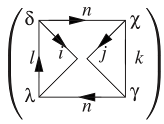

$$\left.\right) \simeq \sum_{\gamma\lambda,p\sigma\epsilon} F^{ijm^*,\alpha\beta}_{kln,\gamma\lambda}F^{ln^*i^*,\delta\lambda}_{nlp^*,\sigma\epsilon}\Phi_{\text{fix}}\left(\right.$$
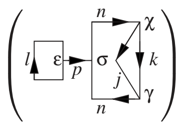

$$\left.\right) \simeq \sum_{\gamma\lambda,p\sigma\epsilon} F^{ijm^*,\alpha\beta}_{kln,\gamma\lambda}F^{ln^*i^*,\delta\lambda}_{nlp^*,\sigma\epsilon}P^{pl^*,\sigma\epsilon}_{n}\Phi_{\text{fix}}\left(\right.$$
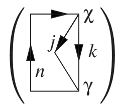

$$\left.\right) = \sum_{\gamma\lambda,p\sigma\epsilon} F^{ijm^*,\alpha\beta}_{kln,\gamma\lambda}F^{ln^*i^*,\delta\lambda}_{nlp^*,\sigma\epsilon}P^{pl^*,\sigma\epsilon}_{n}\Phi^{\theta}_{kjn^*,\gamma\chi}. \tag{49}$$

It is not clear if Eqs. (48) and (49) will lead to new independent equations or not. In the following discussions, we will not include Eqs. (48) and (49). We find that, at least for simple cases, the equations without Eqs. (48) and (49) are enough to completely determine the solutions.

To summarize, the conditions [Eqs. (9), (12), (18), (23), (30), (33), (36), (38), (40), (42), and (44)–(47)] form a set of nonlinear equations whose variables are N_{ijk}, $F^{ijm,\alpha\beta}_{kln,\gamma\lambda}$, $P^{kj,\alpha\beta}_{i}$, A^i, and $(\theta_F,\theta_{P1},\theta_{P2})$. Finding N_{ijk}, $F^{ijm,\alpha\beta}_{kln,\gamma\lambda}$, $P^{kj,\alpha\beta}_{i}$, and A^i that satisfy such a set of nonlinear equations corresponds to finding a fixed-point gLU transformation that has a nontrivial fixed-point wave function. So the solutions $(N_{ijk},F^{ijm,\alpha\beta}_{kln,\gamma\lambda},P^{kj,\alpha\beta}_{i},A^i)$ give us a characterization of topological orders. This may lead to a classification of topological order from the local unitary transformation point of view.

IX. SIMPLE SOLUTIONS OF THE FIXED-POINT CONDITIONS

In this section, let us find some simple solutions of the fixed-point conditions [Eqs. (9), (12), (18), (23), (30), (33), (36), (38), (40), (42), and (44)–(47)] for the fixed-point gLU transformations $(N_{ijk},F^{ijm,\alpha\beta}_{kln,\gamma\lambda},P^{kj,\alpha\beta}_{i})$ and the fixed-point wave function A^i.

A. Unimportant phase factors in the solutions

Formally, the solutions of the fixed-point conditions are not isolated. They are parametrized by several continuous phase factors. In this section, we will discuss the origin of those phase factors. We will see that those different phase factors do not correspond to different states of matter (i.e., different equivalence classes of gLU transformations). So after removing those unimportant phase factors, the solutions of the fixed-point conditions are isolated (at least for the simple examples studied here).

We notice that, apart from two normalization conditions, all of the fixed-point conditions are linear in $P^{kj,\alpha\beta}_{i}$ and A^i. Thus if $(F^{ijm,\alpha\beta}_{kln,\gamma\lambda},P^{kj,\alpha\beta}_{i},A^i)$ is a solution, then $(F^{ijm,\alpha\beta}_{kln,\gamma\lambda},e^{i\phi_1}P^{kj,\alpha\beta}_{i},e^{i\phi_2}A^i)$ is also a solution. However, the two phase factors $e^{i\phi_{1,2}}$ do not lead to different fixed-point wave functions since they only affect the total phase of the wave function and are unphysical. Thus the total phases of P^{kj}_i and A^i can be adjusted. We can use this degree of freedom to set, say, $P^{00,11}_0\geq 0$ and $A^0>0$.

Similarly the total phase of $F^{ijm,\alpha\beta}_{kln,\gamma\lambda}$ is also unphysical and can be adjusted. We have used this degree of freedom to reduce Eq. (17) to Eq. (18). But this does not totally fix the total phase of $F^{ijm,\alpha\beta}_{kln,\gamma\lambda}$. The transformation $F^{ijm,\alpha\beta}_{kln,\gamma\lambda}\to -F^{ijm,\alpha\beta}_{kln,\gamma\lambda}$ does not affect Eq. (18). We can use such a transformation to set the real part of a nonzero component of $F^{ijm,\alpha\beta}_{kln,\gamma\lambda}$ to be positive.

The above three phase factors are unphysical. However, the fixed-point solutions may also contain phase factors that do correspond to different fixed-point wave functions. For example, the local unitary transformation $e^{i\theta_{l_0}\hat{M}_{l_0}}$ does not affect the fusion rule N_{ijk}, where $\hat{M}_{l_0}$ is the number of links with $|l_0\rangle$ state and $|l_0^*\rangle$ state. Such a local unitary transformation changes $(F^{ijm,\alpha\beta}_{kln,\gamma\lambda},P^{kj,\alpha\beta}_{i},A^i)$ and generates a continuous family of the fixed-point wave functions parametrized by θ_{l_0}. Those wave functions are related by local unitary transformations that continuously connect to identity. Thus, those fixed-point wave functions all belong to the same phase.

Similarly, we can consider the following local unitary transformation $|\alpha\rangle\to\sum_\beta U^{(i_0j_0k_0)}_{\alpha\beta}|\beta\rangle$ that acts on each vertex with states $|i_0\rangle,|j_0\rangle,|k_0\rangle$ on the three edges connecting to the vertex. Such a local unitary transformation also does not affect the fusion rule N_{ijk}. The new local unitary transformation changes $(F^{ijm,\alpha\beta}_{kln,\gamma\lambda},P^{kj,\alpha\beta}_{i},A^i)$ and generates a continuous family of the fixed-point wave functions parametrized by the unitary matrix $U^{(i_0j_0k_0)}_{\alpha\beta}$. Again, those fixed-point wave functions all belong to the same phase.

In the following, we will study some simple solutions of the fixed-point conditions. We find that, for those examples, the solutions have no addition continuous parameter apart from the phase factors discussed above. This suggests that the solutions of the fixed-point conditions correspond to isolated zero-temperature phases.

B. $N=1$ loop state

Let us first consider a system where there are only two states $|0\rangle$ and $|1\rangle$ on each link of the graph. We choose i^*

$=i$ and the simplest fusion rule that satisfies Eqs. (9), (30), and (47) is

$$N_{000} = N_{110} = N_{101} = N_{011} = 1,$$

other

$$N_{ijk} = 0. \tag{50}$$

Since $N_{ijk} \leq 1$, there is no states on the vertices. So the indices $\alpha, \beta, \ldots$ labeling the states on a vertex can be suppressed.

The above fusion rule corresponds to the fusion rule for the $N=1$ loop state discussed in Ref. 63. So we will call the corresponding graphic state $N=1$ loop state.

Due to the relation [Eq. (18)], the different components of the tensor F^{ijm}_{kln} are not independent. There are only four independent potentially nonzero components which are denoted as $f_0, \ldots, f_3$:

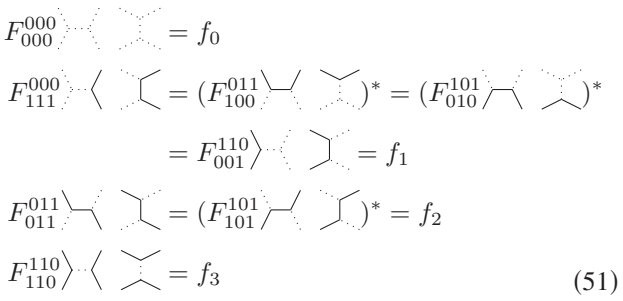

(51)

We note that F^{ijm}_{kln} in Eq. (11) relates wave functions on two graphs. In the above we have drawn the two related graphs after the F tensor, where the first graph following F corresponds to the graph on the left-hand side of Eq. (11) and the second graph corresponds to the graph on the right-hand side of Eq. (11). The doted line corresponds to the $|0\rangle$ state on the link and the solid line corresponds to the $|1\rangle$ state on the link. There are four potentially nonzero components in P^{kj}_i, which are denoted by $p_0, \ldots, p_3$,

$$P^{00}_0 = p_0, \quad P^{01}_0 = p_1, \quad P^{00}_1 = p_2, \quad P^{01}_1 = p_3. \tag{52}$$

We can adjust the total phases of p_i and A^i to make $p_0 \geq 0$ and $A^0 \geq 0$. We can also use the local unitary transformation $e^{i\theta_{l_0}\hat{M}_{l_0}}$ with $l_0=1$ to make $f_1 \geq 0$ since the F's described by f_1 in Eq. (51) are the only F's that change the number of $|1\rangle$ links.

The fixed-point conditions [Eqs. (9), (12), (18), (23), (30), (33), (36), (38), (40), (42), and (44)–(47)] form a set of nonlinear equations on the ten variables f_i, p_i, and A^i. Many of the nonlinear equations are dependent or even equivalent. Using a computer algebraic system, we simplify the set of nonlinear equations. The simplified equations are (after making the phase choice described above)

$$f_0 = f_1 = f_2 = 1, \quad f_3 = \eta,$$

$$p_1 = p_3 = \eta p_0, \quad p_2 = p_0,$$

$$p_0^2 + |p_1|^2 = 1, \quad |p_2|^2 + |p_3|^2 = 1,$$

$$p_1 A^0 = p_2 A^1, \quad \eta p_3 A^1 = p_1 A^0, \quad |A^0|^2 + |A^1|^2 = 1, \tag{53}$$

where $\eta = \pm 1$. The above simplified equations can be solved exactly. We find two solutions parametrized by $\eta = \pm 1$,

$$f_0 = f_1 = f_2 = 1, \quad f_3 = \eta,$$

$$p_0 = p_2 = \frac{1}{\sqrt{2}}, \quad p_1 = p_3 = \frac{\eta}{\sqrt{2}},$$

$$A^0 = \frac{1}{\sqrt{2}}, \quad A^1 = \frac{\eta}{\sqrt{2}}. \tag{54}$$

We also find

$$e^{i\theta_F} = e^{i\theta_{P1}} = e^{i\theta_{P2}} = e^{i\theta_{A1}} = e^{i\theta_{A2}} = 1. \tag{55}$$

The $\eta=1$ fixed-point state corresponds to the $\mathbb{Z}_2$ loop condensed state whose low-energy effective-field theory is the $\mathbb{Z}_2$ gauge theory.[63,66] We call such a state, simply, the $\mathbb{Z}_2$ state. The $\eta=-1$ fixed-point state corresponds to the double-semion state whose low-energy effective-field theory is the $U(1) \times U(1)$ Chern-Simons gauge theory[63,66]

$$\mathcal{L} = \frac{1}{4\pi}(2a_{1\mu}\partial_\nu a_{1\lambda}\epsilon^{\mu\nu\lambda} - 2a_{2\mu}\partial_\nu a_{2\lambda}\epsilon^{\mu\nu\lambda}). \tag{56}$$

C. $N=1$ string-net state

To obtain another class of simple solutions, we modify the fusion rule to

$$N_{000} = N_{110} = N_{101} = N_{011} = N_{111} = 1,$$

other

$$N_{ijk} = 0 \tag{57}$$

while keeping everything the same. The above N_{ijk} also satisfies Eqs. (9), (30), and (47).

The new fusion rule corresponds to the fusion rule for the $N=1$ string-net state discussed in Ref. 63. So we will call the corresponding graphic state $N=1$ string-net state.

Again, due to the relation [Eq. (18)], the different components of the tensor F^{ijm}_{kln} are not independent. Now there are seven independent potentially nonzero components which are denoted as $f_0, \ldots, f_6$,

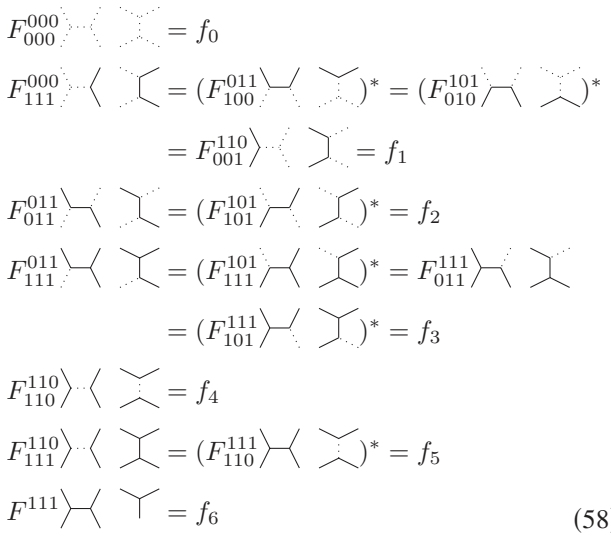

(58)

Note that F's described by f_1 and f_5 are the only F's that change the number of $|1\rangle$ links and the number of $|1\rangle|1\rangle|1\rangle$ vertices. So we can use the local unitary transformation $e^{i(\theta\hat{M}_1+\phi\hat{M}_{111})}$ to make f_1 and f_5 to be positive real numbers. (Here $\hat{M}_1$ is the total number of $|1\rangle$ links and $\hat{M}_{111}$ is the total number of $|1\rangle|1\rangle|1\rangle$ vertices.) We also use the freedom of adjusting the total sign of F^{ijm}_{kln} to make $\mathrm{Re}(f_0)\geq 0$.

There are five potentially nonzero components in P^{kj}_i, which are denoted by $p_0,\ldots,p_4$,

$$P^{00}_0=p_0,\quad P^{01}_0=p_1,\quad P^{00}_1=p_2,$$

$$P^{01}_1=p_3,\quad P^{11}_1=p_4. \tag{59}$$

We use the freedom of adjusting the total phase of P^{kj}_i to make p_0 to be a positive number. We can also use the freedom of adjusting the total phase of A^i to make A^0 to be a positive number.

The fixed-point conditions [Eqs. (12), (18), (23), (33), (36), (38), (40), (42), and (44)–(46)] form a set of nonlinear equation on the variables f_i, p_i, and A^i, which can be simplified. The simplified equations have the following form:

$$f_0=f_1=f_2=f_3=1,\quad f_4=f_5^2=-f_6>0,$$

$$p_1^2f_4^2+p_1^2=1,\quad p_0=f_4p_1,\quad p_2=p_0,\quad p_3=p_1,\quad p_4=0,$$

$$A^0=f_4A^1,\quad (A^0)^2+(A^1)^2=1,\quad f_4^2+f_4-1=0. \tag{60}$$

Let γ be the positive solution of $\gamma^2+\gamma=1$: $\gamma=\frac{\sqrt{5}-1}{2}$. We see that $f_5=\sqrt{\gamma}$. The above can be written as

$$f_0=f_1=f_2=f_3=1,\quad f_4=-f_6=\gamma,\quad f_5=\sqrt{\gamma},$$

$$p_0=p_2=\frac{\gamma}{\gamma^2+1},\quad p_1=p_3=\frac{1}{\gamma^2+1},\quad p_4=0,$$

$$A^0=\frac{\gamma}{\gamma^2+1},\quad A^1=\frac{1}{\gamma^2+1}. \tag{61}$$

We also find

$$e^{i\theta_F}=e^{i\theta_{P1}}=e^{i\theta_{P2}}=e^{i\theta_{A1}}=e^{i\theta_{A2}}=1. \tag{62}$$

The fixed-point state corresponds to the $N=1$ string-net condensed state[63] whose low-energy effective-field theory is the doubled $SO(3)$ Chern-Simons gauge theory.[66]

D. An $N=2$ string-net state—The $\mathbb{Z}_3$ state

The above simple examples correspond to nonorientable string-net states. Here we will give an example of orientable string-net state. We choose $N=2$, $0^*=0$, $1^*=2$, $2^*=1$, and

$$N_{000}=N_{012}=N_{120}=N_{201}=N_{021}=N_{102}=N_{210}=N_{111}=N_{222}=1. \tag{63}$$

The above N_{ijk} satisfies Eqs. (9), (30), and (47).

Due to the relation [Eq. (18)], the different components of the tensor F^{ijm}_{kln} are not independent. There are eight independent potentially nonzero components which are denoted as $f_0,\ldots,f_7$:

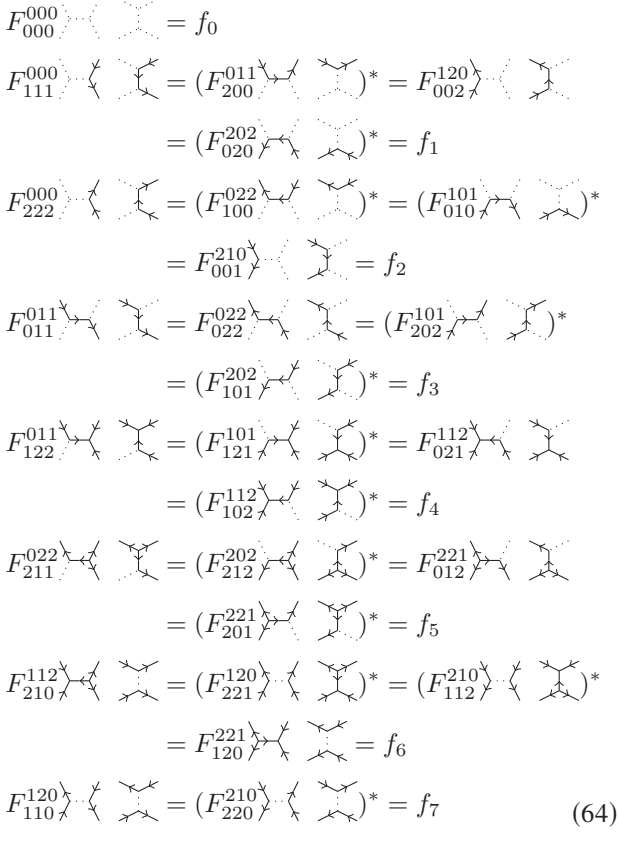

(64)

There are nine potentially nonzero components in P^{kj}_i, which are denoted by $p_0,\ldots,p_8$,

$$P^{00}_0=p_0,\quad P^{01}_0=p_1,\quad P^{02}_0=p_2,\quad P^{00}_1=p_3,\quad P^{01}_1=p_4,$$

$$P^{02}_1=p_5,\quad P^{00}_2=p_6,\quad P^{01}_2=p_7,\quad P^{02}_2=p_8. \tag{65}$$

Using the transformations discussed in Sec. IX B, we can fix the phases of f_1, f_2, f_6, and p_0 to make them positive.

The fixed-point conditions [Eqs. (12), (18), (23), (33), (36), (38), (40), (42), and (44)–(46)] form a set of nonlinear equation on the variables f_i, p_i, and A^i, which can be solved exactly. After fixing the phases using the transformations discussed in Sec. IX B, we find only one solution

$$f_i = 1, \quad i = 0,1,\ldots,7,$$

$$p_i = \frac{1}{\sqrt{3}}, \quad i = 0,1,\ldots,8,$$

$$A^0 = A^1 = A^2 = \frac{1}{\sqrt{3}}. \tag{66}$$

We also find

$$e^{i\theta_F} = e^{i\theta_{P1}} = e^{i\theta_{P2}} = e^{i\theta_{A1}} = e^{i\theta_{A2}} = 1. \tag{67}$$

The fixed-point state corresponds to the $\mathbb{Z}_3$ string-net condensed state[63] whose low-energy effective-field theory is the $U(1)\times U(1)$ Chern-Simons gauge theory[55,63]

$$\mathcal{L} = \frac{1}{4\pi}(3a_{1\mu}\partial_\nu a_{2\lambda}\epsilon^{\mu\nu\lambda} + 3a_{2\mu}\partial_\nu a_{1\lambda}\epsilon^{\mu\nu\lambda}), \tag{68}$$

which is the $\mathbb{Z}_3$ gauge theory.

We note that all the above simple solutions also satisfy the standard pentagon identity, although we solved the weaker projective pentagon identity. It is not clear if we can find nontrivial solutions that do not satisfy the standard pentagon identity.

X. A CLASSIFICATION OF TIME-REVERSAL INVARIANT TOPOLOGICAL ORDERS

There are several ways to define time-reversal operation for the graphic states. The simplest one is given by

$$\hat{T}:\Phi(\Gamma) \to \Phi^*(\Gamma), \tag{69}$$

where Γ represents the labels on the vertices and links which are not changed under $\hat{T}$. (This corresponds to the situation where the different states on the links and the vertices are realized by different occupations of scalar bosons.) For such a time reversal transformation, $\hat{T}^2=1$ and the real solutions of the fixed-point conditions [Eqs. (9), (12), (18), (23), (30), (33), (36), (38), (40), (42), and (44)–(46)] give us a classification of time reversal invariant topological orders in local spin systems. Note that the time-reversal invariant topological orders are equivalent class of local orthogonal transformations that connect to the identity transformation continuously.

Different real solutions $(N_{ijk}, F^{ijm,\alpha\beta}_{kln,\gamma\lambda}, P_i^{kj,\alpha\beta}, A^i)$ of the fixed-point conditions do not always correspond to different time-reversal invariant topological orders. The solutions differ by some unimportant phase factors (which are ± 1 signs) correspond to the same topological order.

To understand the above result, we notice that, from the structure of the fixed-point conditions, if $(F^{ijm,\alpha\beta}_{kln,\gamma\lambda}, P_i^{kj,\alpha\beta}, A^i)$ is a solution, then $(\eta_F F^{ijm,\alpha\beta}_{kln,\gamma\lambda}, \eta_P P_i^{kj,\alpha\beta}, \eta_A A^i)$ is also a solution, where $\eta_F = \pm 1$, $\eta_P = \pm 1$, and $\eta_A = \pm 1$. However, the three phase factors η_F, η_P, and η_A do not lead to different fixed-point wave functions since they only affect the total phase of the wave function and are unphysical.

On the other hand, the fixed-point solutions may also contain phase factors that do correspond to different fixed-point wave functions. For example, the local orthogonal transformation $e^{i\pi\hat{M}_{l_0}}$ does not affect the fusion rule N_{ijk}, where $\hat{M}_{l_0}$ is the number of links with $|l_0\rangle$ state and $|l_0^*\rangle$ state. Such a local orthogonal transformation changes $(F^{ijm,\alpha\beta}_{kln,\gamma\lambda}, P_i^{kj,\alpha\beta}, A^i)$ and generates a discrete family of the fixed-point wave functions.

Similarly, we can consider the following local orthogonal transformation $|\alpha\rangle \to \Sigma_\beta O^{(i_0 j_0 k_0)}_{\alpha\beta}|\beta\rangle$ that acts on each vertex with states $|i_0\rangle, |j_0\rangle, |k_0\rangle$ on the three edges connecting to the vertex. Such a local orthogonal transformation also does not affect the fusion rule N_{ijk}. The new local orthogonal transformation changes $(F^{ijm,\alpha\beta}_{kln,\gamma\lambda}, P_i^{kj,\alpha\beta}, A^i)$ and generates a family of the fixed-point wave functions parametrized by the orthogonal matrix $O^{(i_0 j_0 k_0)}_{\alpha\beta}$.

Now the question is that do those solutions related by local orthogonal transformations have the same time-reversal invariant topological order or not. We know that two gapped wave functions have the same time-reversal invariant topological order if and only if they can be connected by local orthogonal transformation that *connects to identity continuously*. It is well known that an orthogonal matrix whose determinant is -1 does not connect to identity. Thus it appears that local orthogonal transformations some times can generate different time reversal invariant topological orders.

However, when we use the equivalent classes of local orthogonal transformations to define time-reversal invariant topological orders, we not only assume the local orthogonal transformations to connect to identity continuously, we also assume that we can expand the local Hilbert spaces (say by increasing the range of the indices i and α that label the states on the edges and the vertices). The local orthogonal transformations can act on those enlarged Hilbert spaces and can connect to identity in those enlarged Hilbert spaces. Even when a local orthogonal transformation cannot be deformed into identity in the original Hilbert space, it can always be deformed into identity continuously in an enlarged Hilbert space. Thus two real wave functions related by a local orthogonal transformation always have the same time-reversal invariant topological order.

For example, an orthogonal matrix $\left(\begin{smallmatrix}1 & 0\\ 0 & -1\end{smallmatrix}\right)$ that acts on states $|0\rangle$ and $|1\rangle$ does not connect to identity within the space of two by two orthogonal matrices. However, we can embed the above orthogonal matrix into a three by three orthogonal matrix that acts on $|0\rangle$, $|1\rangle$, and $|2\rangle$:

$$\begin{pmatrix} 1 & 0 & 0 \\ 0 & -1 & 0 \\ 0 & 0 & -1 \end{pmatrix}.$$

Such a three by three orthogonal matrix does connect to identity within the space of three by three orthogonal matrices. This completes our argument that all local orthogonal transformations can connect to identity continuously at least in an enlarged Hilbert space.

So, after factoring out the unimportant phase factors discussed above, the real solutions of the fixed-point conditions may uniquely correspond to time-reversal invariant topological orders. The four types of real solutions discussed in the

last section are examples of four different time-reversal invariant topological orders.

For the $N=1$ loop states and the $N=1$ string-net state, we only have two states on each link. In this case, we can treat the two states as the two states of an electron spin. The time-reversal transformation now becomes

$$\hat{T}: c_0|0\rangle + c_1|1\rangle \to -c_1^*|0\rangle + c_0^*|1\rangle \tag{70}$$

on each link. For such a time-reversal transformation $\hat{T}^2=-1$. The two $N=1$ loop states and the $N=1$ string-net state are not invariant under such a time-reversal transformation.

XI. WAVE FUNCTION RENORMALIZATION FOR TENSOR PRODUCT STATES

A. Motivation

Once the fixed-point states have been identified and the labeling of topological orders has being found, we then face the next important issue: given a generic ground-state wave function of a system, how to identify the topological orders in the state? In other words, how to calculate the data $(N_{ijk}, F_{kln,\gamma\lambda}^{ijm,\alpha\beta}, P_i^{kj,\alpha\beta}, A^i)$ that characterize the topological orders from a generic wave function?

One way to address the above issue is to have a general renormalization procedure which flows other states in the same phase to the simple fixed-point state so that we can identify topological order from the resulting fixed-point state. That is, we want to find a local unitary transformation which removes local entanglement and gets rid of unnecessary degrees of freedom from the state. How to find the appropriate unitary transformation for a specific state is then the central problem in this renormalization procedure. Such a procedure for one-dimensional tensor product states (TPS) (also called matrix product states) has been given in Ref. 42. Here we will propose a method to renormalize two-dimensional TPS, where nontrivial topological orders emerge. The basic idea is to use the gLU transformation discussed in Sec. VII. Note that, through the gLU transformation, we can reduce the number of labels in a region A to the minimal value without loosing any quantum information (see Fig. 6). This is because the gLU transformation is a lossless projection into the support space of the state in the region A. By performing such gLU transformations on *overlapping* regions repeatedly [see Fig. 2(a)], we can reduce a generic wave function to the simple fixed-point form discussed above. It should be noted that any state reducible in this way can be represented as a MERA.[43]

In the following, we will present this renormalization procedure for two-dimensional TPS where we find a method to calculate the proper gLU transformations. The tensor product states are many-body entangled quantum states described with local tensors. By making use of the entanglement information contained in the local tensors, we are able to come up with an efficient algorithm to renormalize two-dimensional TPS.

This algorithm can be very useful in the study of quantum phases. Due to the efficiency in representation, TPS has found wide application as variational ansatz states in the studies of quantum many-body systems.[67–73] Suppose that in a variational study we have found a set of tensors which describe the ground state of a two-dimensional many-body Hamiltonian and want to determine the phase this state belongs to. We can apply our renormalization algorithm to this tensor product state, which removes local entanglement and flows the state to its fixed point. By identifying the kind of order present in the fixed-point state, we can obtain the phase information for the original state.

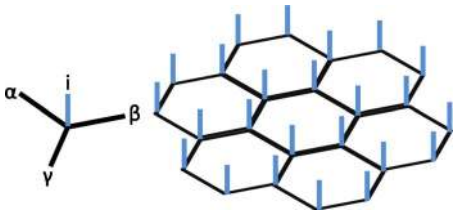

FIG. 11. (Color online) Left: tensor T representing a 2D quantum state on hexagonal lattice. i is the physical index and α, β, γ are the inner indices. Right: a tensor product state where each vertex is associated with a tensor. The inner indices of the neighboring tensors connect according to the underlying hexagonal lattice.

In this section, we will give a detailed description of the algorithm and in the next section we will present its application to some simple (but nontrivial) cases. The states we are concerned with have translational symmetry and can be described with a translational invariant tensor network. To be specific, we discuss states on a hexagonal lattice. Generalization to other regular lattices is straightforward.

B. Tensor product states

Consider a two-dimensional spin model on a hexagonal lattice with one spin (or one qudit) living at each vertex. The Hilbert space of each spin is D dimensional. The state can be represented by assigning to every vertex a set of tensors $T^i_{\alpha\beta\gamma}$, where i (see Fig. 11) labels the local physical dimension and takes value from 1 to D. α, β, γ are inner indices along the three directions in the hexagonal lattice, respectively. The dimension of the inner indices is d. Note that the figures in this note are all sideviews with inner indices in the horizontal plane and the physical indices pointing in the vertical direction, if not specified otherwise.

The wave function is given in terms of these tensors by

$$|\psi\rangle = \sum_{i_1,i_2,\ldots,i_m,\ldots} \mathrm{tTr}(T^{i_1}T^{i_2},\ldots,T^{i_m},\ldots)|i_1 i_2,\ldots,i_m,\ldots\rangle, \tag{71}$$

where tTr denotes tensor contraction of all the connected inner indices on the links of the hexagonal lattice.

A renormalization procedure of quantum states is composed of local unitary transformations and isometry maps such that the state flows along the path $|\psi^{(0)}\rangle, |\psi^{(1)}\rangle, |\psi^{(2)}\rangle, \ldots$ and finally toward a fixed point $|\psi^{\infty}\rangle$. With the tensor product representation, flow of states corresponds to a flow of tensors $T^{(0)}, T^{(1)}, T^{(2)}, \ldots$ We will give the detailed procedure of how the tensors are mapped from one step to the next in the following section.

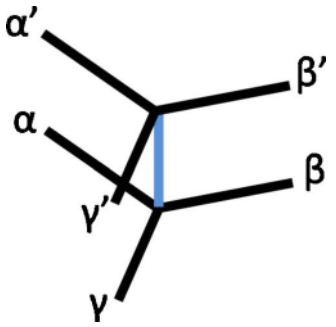

FIG. 12. (Color online) Double tensor $\mathbb{T}$ represented as two layers of tensor T with the physical indices contracted. The gray layer is the lower layer.

C. Renormalization algorithm

In one round of renormalization, we start from tensor $T^{(n)}$, do some operation to it which corresponds to local unitary transformations on the state, and map $T^{(n)}$ to $T^{(n+1)}$. The whole procedure can be broken into two parts: the F-move and the P move, in accordance with the two steps introduced in the previous section.

1. Step 1: F-move

In the F-move, we take a

configuration in the tensor network and map it to a

configuration by doing a local unitary operation. We will see that the tensor product representation of a state leads to a natural way of choosing an appropriate unitary operation for the renormalization of the state.

In order to do so, first we define the double tensor $\mathbb{T}$ of tensor T as

$$\mathbb{T}_{\alpha'\beta'\gamma',\alpha\beta\gamma} = \sum_i (T^i_{\alpha'\beta'\gamma'})^* \times T^i_{\alpha\beta\gamma}. \tag{72}$$

Graphically the double tensor $\mathbb{T}$ is represented by two layers of tensor T with the physical indices connected (see Fig. 12). The tensor T giving rise to the same double tensor $\mathbb{T}$ is not unique. Any tensor T' which differs from T by an unitary transformation U on physical index i gives the same $\mathbb{T}$ as U and $U^\dagger$ cancels out in the contraction of i. On the other hand, an unitary transformation on i is the only degree of freedom possible, i.e., any T' which gives rise to the same $\mathbb{T}$ as T differs from T by a unitary on i. Therefore, in the process of turning a tensor T into a double tensor $\mathbb{T}$ and then split it again into a different tensor T', we apply a nontrivial local unitary operation on the corresponding state. A well designed way of splitting the double tensor will give us the appropriate unitary transformation we need, as we show below.

F-move has the following steps. First, construct double tensors for two neighboring sites on the lattice and combine them into a single double tensor with eight inner indices.

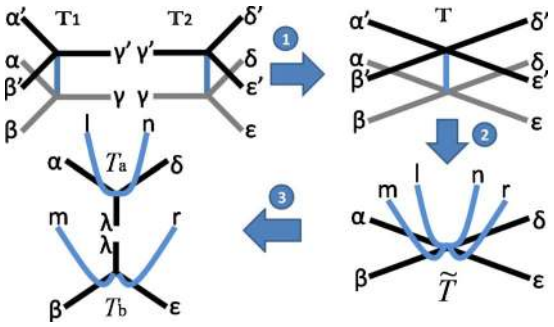

FIG. 13. (Color online) F-move in the renormalization procedure: (1) combining double tensors $\mathbb{T}_1$ and $\mathbb{T}_2$ on neighboring sites into a single double tensor $\mathbb{T}$, (2) splitting double tensor $\mathbb{T}$ into tensor $\tilde{T}$, and (3) SVD decomposition of tensor $\tilde{T}$ into tensors T_a and T_b.

$$\mathbb{T}_{\alpha'\beta'\delta'\epsilon',\alpha\beta\delta\epsilon} = \sum_{\gamma',\gamma} \mathbb{T}_{1,\alpha'\beta'\gamma',\alpha\beta\gamma} \times \mathbb{T}_{2,\delta'\epsilon'\gamma',\delta\epsilon\gamma}. \tag{73}$$

Note that with respect to the bipartition of indices $\alpha'\beta'\delta'\epsilon'$ and $\alpha\beta\delta\epsilon$, $\mathbb{T}$ is Hermitian

$$\mathbb{T}_{\alpha'\beta'\delta'\epsilon',\alpha\beta\delta\epsilon} = (\mathbb{T}_{\alpha\beta\delta\epsilon,\alpha'\beta'\delta'\epsilon'})^* \tag{74}$$

and positive semidefinite. Therefore it has a spectral decomposition with positive eigenvalues $\{\lambda_j \geq 0\}$. The corresponding eigenvectors are $\{\hat{T}^j\}$,

$$\mathbb{T}_{\alpha'\beta'\delta'\epsilon',\alpha\beta\delta\epsilon} = \sum_j \lambda_j (\hat{T}^j_{\alpha'\beta'\delta'\epsilon'})^* \times \hat{T}^j_{\alpha\beta\delta\epsilon}. \tag{75}$$

This spectral decomposition lead to a special way of decomposing double tensor $\mathbb{T}$ into tensors. Define a rank 8 tensor $\tilde{T}$(as shown in Fig. 13 after step 2) as follows:

$$\tilde{T}^{lmnr}_{\alpha\beta\delta\epsilon} = \sum_j \sqrt{\lambda_j} (\hat{T}^j_{lmnr})^* \times \hat{T}^j_{\alpha\beta\delta\epsilon}. \tag{76}$$

$\tilde{T}$ has four inner indices $\alpha,\beta,\delta,\epsilon$ of dimension d and four physical indices l,m,n,r also of dimension d which are in the direction of $\alpha,\beta,\delta,\epsilon$, respectively. As $\{\hat{T}^j\}$ form an orthonormal set, it is easy to check that $\tilde{T}$ gives rise to double tensor $\mathbb{T}$. Going from T_1 and T_2 to $\tilde{T}$, we have implemented a local unitary transformation on the physical degrees of freedom on the two sites so that in $\tilde{T}$ the physical indices and the inner indices represent the same configuration. In some sense, we are keeping only the physical degrees of freedom necessary for entanglement with the rest of the system while getting rid of those that are only entangled within this local region. Now we do a singular value decomposition of tensor $\tilde{T}$ in the direction orthogonal to the link between T_1 and T_2 and $\tilde{T}$ is decomposed into tensors T_a and T_b,

$$\tilde{T}^{lmnr}_{\alpha\beta\delta\epsilon} = \sum_\lambda T^{ln}_{a,\alpha\delta\lambda} \times T^{mr}_{b,\beta\epsilon\lambda}. \tag{77}$$

This step completes the F-move. Ideally, this step should be done exactly so we are only applying local unitary operations to the state. Numerically, we keep some large but finite cut-

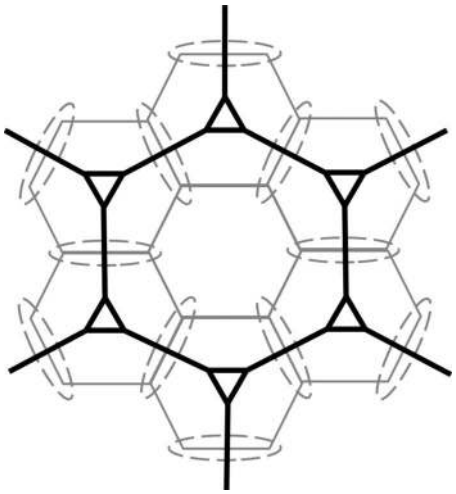

FIG. 14. Original hexagonal lattice (gray line) and renormalized lattice (black line) after F-move has been applied to the neighboring pairs of sites circled by dash line.

off dimension for the singular value decomposition step, so this step is approximate.

On a hexagonal lattice, we do F-move on the chosen neighboring pairs of sites (dash circled in Fig. 14) so that the tensor network is changed into a configuration shown by thick dark lines in Fig. 14. Physical indices are omitted from this figure. Now by grouping together the three tensors that meet at a triangle, we can map the tensor network back into a hexagonal lattice, with 1/3 the number of sites in the original lattice. This is achieved by the P-move introduced in the next section.

2. Step 2: P-move

Now we contract the three tensors that meet at a triangle together to form a new tensor in the renormalized lattice as shown in the first step in Fig. 15,

$$T^{I}_{\alpha\beta\gamma} = \sum_{\delta\epsilon\lambda} T^{nr}_{a,\alpha\delta\epsilon} \times T^{lm}_{b,\beta\lambda\delta} \times T^{pq}_{c,\gamma\epsilon\lambda}, \tag{78}$$

where I is the physical index of the new tensor which includes all the physical indices of T_a, T_b, T_c: l, m, n, r, p, q. Note that in the contraction, only inner indices are contracted and the physical indices are simply group together. Constructing the double tensor $\mathbb{T}$ from T, we get the renormalized double tensor on the new hexagonal lattice which is in

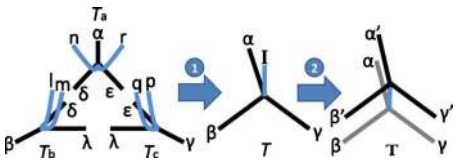

FIG. 15. (Color online) P-move in the renormalization procedure: (1) contracting three tensors that meet at a triangle T_a, T_b, T_c to form a new tensor $T^{(1)}$ on one site of the renormalized hexagonal lattice. (2) Constructing the double tensor $\mathbb{T}^{(1)}$ from $T^{(1)}$ so that we can start to do F-moves again.

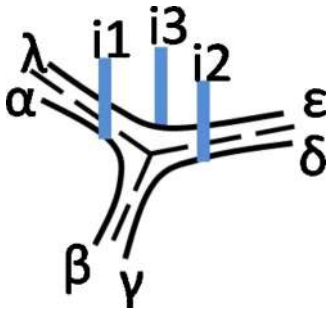

FIG. 16. (Color online) The corner double line tensor which is a fixed point of the renormalization algorithm. The three groups of indices $\{\alpha, \beta, i_1\}$, $\{\gamma, \delta, i_2\}$, and $\{\epsilon, \lambda, i_3\}$ are entangled within each group but not between the groups.

the same form as $\mathbb{T}_1, \mathbb{T}_2$ and we can go back again and do the F-move.

3. Complications: Corner double line

One problem with the above renormalization algorithm is that, instead of having one isolated fixed-point tensor for each phase, the algorithm has a continuous family of fixed points which all correspond to the same phase. Consider a tensor with structure shown in Fig. 16. The tensor is a tensor product of three parts which include indices $\{\alpha, \beta, i_1\}$, $\{\gamma, \delta, i_2\}$, and $\{\epsilon, \lambda, i_3\}$, respectively. It can be shown that this structure remains invariant under the renormalization flow. Therefore, any tensor of this structure is a fixed point of our renormalization flow. However, it is easy to see that the state it represents is a tensor product of loops around each plaquette, which can be disentangled locally into a trivial product state. Therefore, the states all have only short-range entanglement and correspond to the topologically trivial phase. The trivial phase has then a continuous family of fixed-point tensors. This situation is very similar to that discussed in Refs. 41 and 74. We will keep the terminology and call such a tensor a corner double line tensor. Not only does corner double line tensor complicate the situation in the trivial phase, it leads to a continuous family of fixed points in every phase. It can be checked that the tensor product of a corner double line with any other fixed-point tensor is still a fixed-point tensor. The states they correspond to differ only by small loops around each plaquette and represent the same topological order. Therefore any single fixed-point tensor gets complicated into a continuous class of fixed-point tensors. In practical application of the renormalization algorithm, in order to identify the topological order of the fixed-point tensor, we need to get rid of such corner double line structures. Due to their simple structure, this can always be done, as discussed in the next section.

XII. APPLICATIONS OF THE RENORMALIZATION FOR TENSOR PRODUCT STATES

Now we present some examples where our algorithm is used to determine the phase of a tensor product state. The algorithm can be applied both to symmetry breaking phases and topological ordered phases. In the study of symmetry

breaking/topological ordered phases, suppose that we have obtained some tensor product description of the ground state of the system Hamiltonian. We can then apply our algorithm to the tensors, flow them to the fixed point, and see whether they represent a state in the symmetry-breaking phase/topological ordered phase or a trivial phase.

For system with symmetry/topological order related to gauge symmetry, it is very important to keep the symmetry/gauge symmetry in the variational approach to ground state and search within the set of tensors that have this symmetry/gauge symmetry.[75] The resulting tensor will be invariant under such symmetries/gauge symmetries but the state they correspond to may have different orders. In the symmetry-breaking case, the state could have this symmetry or could spontaneous break it. In the topological ordered phase, the state could have nontrivial topological order or be just trivial. Our algorithm can then be applied to decide which is the case. In order to correctly determine the phase for such symmetric tensors, it is crucial that we maintain the symmetry/gauge symmetry of the tensor throughout our renormalization process. We will discuss in detail two cases: the Ising symmetry-breaking phase and the $\mathbb{Z}_2$ topological ordered phase. For simplicity of discussion and to demonstrate the generality of our renormalization scheme, we will first introduce the square lattice version of the algorithm. All subsequent applications are carried out on square lattice. (Algorithm on a hexagonal lattice would give qualitatively similar result, though quantitatively they might differ, e.g., on the position of critical point.)

A. Renormalization on square lattice

Tensor product states on a square lattice are represented with one tensor $T^i_{\alpha\beta\gamma\delta}$ on each vertex, where i is the physical index and $\alpha\beta\gamma\delta$ are the four inner indices in the up, down, left, right directions, respectively. We will assume translational invariance and require the tensor to be the same on every vertex. The renormalization procedure is be a local unitary transformation on the state which flows the form of the tensor until it reaches the fixed point. It is implemented in the following steps. First, we form the double tensor $\mathbb{T}$ from tensor T,

$$\mathbb{T}_{\alpha'\beta'\gamma'\delta',\alpha\beta\gamma\delta} = \sum_i (T^i_{\alpha'\beta'\gamma'\delta'})^* \times T^i_{\alpha\beta\gamma\delta}.$$

Then do the spectral decomposition of positive operator $\mathbb{T}$ into

$$\mathbb{T}_{\alpha'\beta'\gamma'\delta',\alpha\beta\gamma\delta} = \sum_j \lambda_j (\hat{T}^j_{\alpha'\beta'\gamma'\delta'})^* \times \hat{T}^j_{\alpha\beta\gamma\delta}$$

and form a new tensor $\tilde{T}^{lmnr}_{\alpha\beta\gamma\delta}$

$$\tilde{T}^{lmnr}_{\alpha\beta\gamma\delta} = \sum_j \sqrt{\lambda_j} (\hat{T}^j_{lmnr})^* \times \hat{T}^j_{\alpha\beta\gamma\delta},$$

where l,m,n,r are physical indices in the up, down, left, and right directions, respectively. This is illustrated in step 1 of Fig. 17. This step is very similar to the second step in the F-move on hexagonal lattice. Next we do SVD decomposition of tensor $\tilde{T}$. For vertices in sublattice A we decompose between the up-right and down-left directions as shown in step 2 of Fig. 17. For vertices in sublattice B we decompose between the up-left and down-right directions as shown in step 3 of Fig. 17,

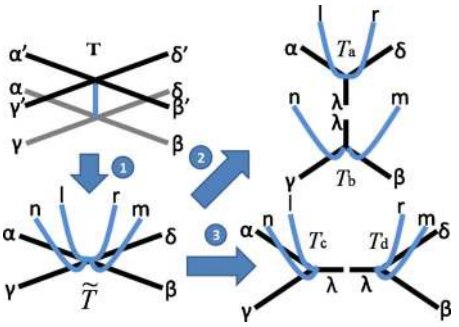

FIG. 17. (Color online) Renormalization procedure on square lattice part 1: (1) decomposing double tensor $\mathbb{T}$ into tensor $\tilde{T}$ and (2) SVD decomposition of $\tilde{T}$ in two different directions, resulting in tensors T_a, T_b and T_c, T_d, respectively.

$$\tilde{T}^{lmnr}_{\alpha\beta\gamma\delta} = \sum_\lambda T^{lr}_{a,\alpha\delta\lambda} \times T^{mn}_{b,\beta\gamma\lambda},$$

$$\tilde{T}^{lmnr}_{\alpha\beta\gamma\delta} = \sum_\lambda T^{lr}_{c,\alpha\delta\lambda} \times T^{mn}_{b,\beta\gamma\lambda}.$$

After the decomposition, the original lattice (gray lines in Fig. 18) is transformed into the configuration shown by thick dark lines in Fig. 18. Physical indices are omitted from this figure. If we now shrink the small squares, we get a tensor product state on a renormalized square lattice. Figure 19 shows how this is done.

In step 1, we contract the four tensors that meet at a small square

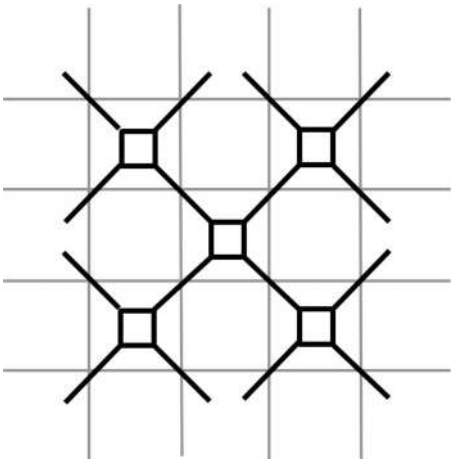

FIG. 18. Original square lattice (gray line) and renormalized lattice (black line) after the operations in Fig. 17 has been applied. Physical indices of the tensors are not drawn here.

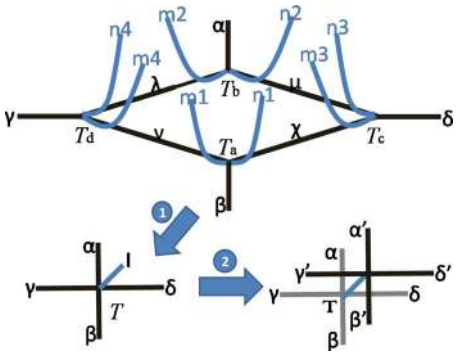

FIG. 19. (Color online) Renormalization procedure on square lattice part 2: (1) combining four tensors that meet at a square into a single tensor and (2) constructing a double tensor from it.

$$T^{I}_{\alpha\beta\gamma\delta} = \sum_{\lambda\mu\nu\chi} T^{m_1 n_1}_{a,\beta\nu\chi} \times T^{m_2 n_2}_{b,\alpha\lambda\mu} \times T^{m_3 n_3}_{c,\delta\mu\chi} \times T^{m_4 n_4}_{d,\gamma\lambda\nu},$$

where I stands for the combination of all physical indices m_i, n_i, $i=1,\ldots,4$. In step 2, we construct a double tensor $\mathbb{T}$ form tensor T and completes one round of renormalization. Now we can go back to step 1 in Fig. 17 and flow the tensor further.

Now we are ready to discuss two particular examples, the Ising symmetry-breaking phase and the $\mathbb{Z}_2$ topological ordered phase, to demonstrate how our algorithm can be used to determine the phase of a tensor product state.

B. Ising symmetry-breaking phase

A typical example for symmetry-breaking phase transition is the transverse field Ising model. Consider a square lattice with one spin 1/2 on each site. The transverse field Ising model is

$$H_{Ising} = \sum_{ij} Z_i Z_j + \epsilon \sum_k X_k,$$

where $\{ij\}$ are nearest-neighbor sites. The Hamiltonian is invariant under spin-flip transformation $\Pi_k X_k$ for any ϵ.

When $\epsilon=0$, the ground state spontaneously breaks this symmetry into either the all spin-up state $|00\cdots0\rangle$ or the all spin-down state $|11\cdots1\rangle$. In this case any global superposition $\alpha|00\cdots0\rangle+\beta|11\cdots1\rangle$ represents a degenerate ground state. When $\epsilon=\infty$, the ground state has all spin polarized in the X direction ($|++\cdots+\rangle$) and does not break this symmetry.

In the variational study of this system, we can require that the variational ground state always have this symmetry, regardless if the system is in the symmetry-breaking phase or not. Then we will find for $\epsilon=0$ the ground state to be $|00\cdots0\rangle+|11\cdots1\rangle$. Such a global superposition represents the spontaneous symmetry breaking. For $\epsilon=\infty$, we will find the ground state to be $|++\cdots+\rangle$ and does not break the symmetry. For $0<\epsilon<\infty$, we will need to decide which of the previous two cases it belongs to. We can first find a tensor product representation of an approximate ground state which is symmetric under the spin-flip transformation, then apply the renormalization algorithm to find the fixed point and decide which phase the state belongs to. Below we will assume a simple form of tensor and demonstrate how the algorithm works.

Suppose that the tensors obtained from the variational study $T^{i}_{\alpha\beta\gamma\delta}$, where $i,\alpha,\beta,\gamma,\delta$ can be 0 or 1, takes the following form:

$$T^{0}_{\alpha\beta\gamma\delta} = \lambda^{\alpha+\beta+\gamma+\delta},$$

$$T^{1}_{\alpha\beta\gamma\delta} = \lambda^{4-(\alpha+\beta+\gamma+\delta)}. \tag{79}$$

λ is a parameter between 0 and 1. Under an X operation to the physical index, the tensor is changed to $\tilde{T}$,

$$\tilde{T}^{0}_{\alpha\beta\gamma\delta} = \lambda^{4-(\alpha+\beta+\gamma+\delta)},$$

$$\tilde{T}^{1}_{\alpha\beta\gamma\delta} = \lambda^{\alpha+\beta+\gamma+\delta}.$$

$\tilde{T}$ can be mapped back to T by switching the 0,1 label for the four inner indices $\alpha\beta\gamma\delta$. Such a change in basis for the inner indices does not change the contraction result of the tensor and hence the state that is represented. Therefore, the state is invariant under the spin-flip transformation $\Pi_k X_k$ and we will say that the tensor has this symmetry also.

When $\lambda=0$, the tensor represents state $|00\cdots0\rangle+|11\cdots1\rangle$, which corresponds to the spontaneous symmetry-breaking phase. We note that the $\lambda=0$ tensor is a direct sum of dimension-1 tensors. Such a direct-sum structure corresponds to spontaneous symmetry breaking, as discussed in detail in Ref. 41. When $\lambda=1$, the tensor represents state $|++\cdots+\rangle$ which corresponds to the symmetric phase. When $0<\lambda<1$, there must be a phase transition between the two phases. However, as λ goes from 0 to 1, the tensor varies smoothly with well-defined symmetry. It is hard to identify the phase-transition point. Now we can apply our algorithm to the tensor. First, we notice that at $\lambda=0$ or 1, the tensor is a fixed point for our algorithm. Next, we find that for $\lambda<0.358$, the tensor flows to the form with $\lambda=0$ while for $\lambda>0.359$, it flows to the form with $\lambda=1$. Therefore, we can clearly identify the phase a state belongs to using this algorithm and find the phase-transition point.

Note that in our algorithm, we explicitly keep the spin-flip symmetry in the tensor. That is, after each renormalization step, we make sure that the renormalized tensor is invariant under spin-flip operations up to change in basis for the inner indices. If the symmetry is not carefully preserved, we will not be able to tell the two phases apart.

We also need to mention that for arbitrary λ, the fixed point that the tensor flows to can be different from the tensor at $\lambda=0$ or 1 by a corner double line structure. We need to get rid of the corner double line structure in the result to identify the real fixed point. This is possible by carefully examining the fixed-point structure. Another way to distinguish the different fixed points without worrying about corner double lines is to calculate some quantities from the fixed-point tensors that are invariant with the addition of corner double lines. We also want the quantity to be invariant under some trivial changes to the fixed point, such as a change in scale $T\to\eta T$ or the change in basis for physical and inner indices. One such quantity is given by the ratio of X_2 and X_1 defined as $X_1=(\Sigma_{\alpha'\gamma',\alpha\gamma}\mathbb{T}_{\alpha'\alpha'\gamma'\gamma',\alpha\alpha\gamma\gamma})^2$ and X_2

FIG. 20. Quantity X_2/X_1 obtained by taking the ratio of the contraction value of the double tensor in two different ways. X_2/X_1 is invariant under change in scale, basis transformation and corner double line structures of the double tensor and can be used to distinguish different fixed-point tensors. For clarity, only one layer of the double tensor is shown. The other layer connects in exactly the same way.

$=\Sigma_{\alpha'\beta'\gamma'\delta',\alpha\beta\gamma\delta}\mathbb{T}_{\alpha'\alpha'\gamma'\delta',\alpha\alpha\gamma\delta}\times\mathbb{T}_{\beta'\beta'\delta'\gamma',\beta\beta\delta\gamma}$. Figure 20 gives a graphical representation of these two quantities. In this figure, only one layer of the double tensor is shown. The other layer connects in the exactly the same way. It is easy to verify that X_2/X_1 is invariant under the change in scale, basis transformation, and corner double lines.

We calculate X_2/X_1 along the renormalization flow. The result is shown in Fig. 21. At the $\lambda=0$ fixed point, $X_2/X_1=0.5$ while at $\lambda=1$, $X_2/X_1=1$. As we increase the number of renormalization steps, the transition between the two fixed points becomes sharper and finally approaches a step function with critical point at $\lambda_c=0.358$. Tensors with $\lambda<\lambda_c$ belongs to the symmetry-breaking phase while tensors with $\lambda>\lambda_c$ belongs to the symmetric phase.

C. $\mathbb{Z}_2$ topological ordered phase

The algorithm can also be used to study topological order of quantum states. In this section, we will demonstrate how the algorithm works with $\mathbb{Z}_2$ topological order.

Consider again a square lattice but now with one spin 1/2 per each link. A simple Hamiltonian on this lattice with $\mathbb{Z}_2$ topological order can be defined as

$$H_{\mathbb{Z}_2}=\sum_p \prod_{i\in p} X_i+\sum_v \prod_{j\in v} Z_j,$$

where p means plaquettes and $i\in p$ is all the spin 1/2's around the plaquette and v means vertices and $j\in v$ is all the spin 1/2's connected to the vertex. The ground-state wave function of this Hamiltonian is a fixed-point wave function and corresponds to the $N=1$ loop state with $\eta=1$ as discussed in the previous section.

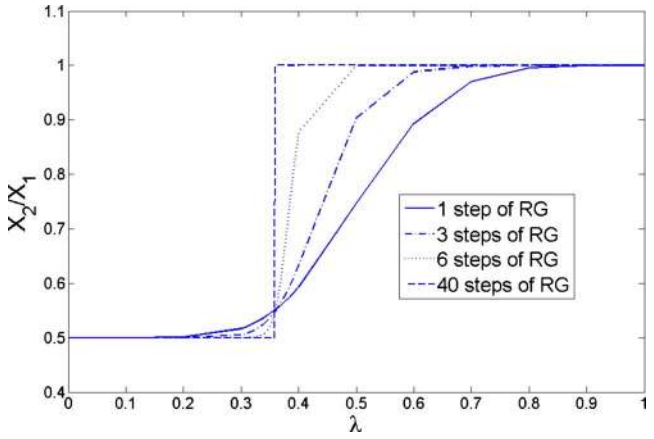

FIG. 21. (Color online) X_2/X_1 for tensors [Eq. (79)] under the renormalization flow. As the number of RG steps increases, the transition in X_2/X_1 becomes sharper and finally approaches a step function at fixed point. The critical point is at $\lambda_c=0.358$.

The ground-state wave function has a simple tensor product representation. For simplicity of discussion we split every spin 1/2 into two and associate every vertex with four spins. The tensor $T^{ijkl}_{\alpha\beta\gamma\delta,\mathbb{Z}_2}$ has four physical indices $i,j,k,l=0,1$ and three inner indices $\alpha,\beta,\gamma,\delta=0,1$.

$$T^{ijkl}_{ijkl,\mathbb{Z}_2}=1, \quad \text{if } \mathrm{mod}(i+j+k+l,2)$$
$$=0 \quad \text{all other terms being } 0.$$

It can be checked that $T_{\mathbb{Z}_2}$ is a fixed-point tensor of our algorithm. This tensor has a $\mathbb{Z}_2$ gauge symmetry. If we apply Z operation to all the inner indices, where Z maps 0 to 0 and 1 to -1, the tensor remains invariant as only even configurations of the inner indices are nonzero in the tensor.

Consider then the following set of tensor parametrized by g

$$T^{ijkl}_{ijkl}=g^{i+j+k+l}, \quad \text{if } \mathrm{mod}(i+j+k+l,2)$$
$$=0 \quad \text{all other terms being } 0. \tag{80}$$

At $g=1$, this is exactly $T_{\mathbb{Z}_2}$ and the corresponding state has topological order. At $g=0$, the tensor represents a product state of all 0 and we denote the tensor as T_0. At some critical point in g, the state must go through a phase transition. This set of tensors are all invariant under gauge transformation $ZZZZ$ on their inner indices and the tensor seems to vary smoothly with g. One way to detect the phase transition is to apply our algorithm. We find that, at $g>g_c$, the tensors flow to $T_{\mathbb{Z}_2}$ while at $g<g_c$, the tensors flow to T_0. We determine g_c to be between 0.804 and 0.805. As this model is mathematically equivalent to two-dimensional classical Ising model where the transition point is known to great accuracy, we compare our result to that result and find our result to be within 1% accuracy ($g_c=0.8022$). Again in the renormalization algorithm, we need to carefully preserve the $\mathbb{Z}_2$ gauge symmetry of the tensor so that we can correctly determine the phase of the states.

The fixed-point tensor structure might also be complicated by corner double line structures but it is always possible to identify and get rid of them. Similarly, we can calculate the invariance quantity X_2/X_1 to distinguish the two fixed points. $X_2/X_1=1$ for $T_{\mathbb{Z}_2}$ while $X_2/X_1=0.5$ for T_0. The result is plotted in Fig. 22 and we can see that the transition in X_2/X_1 approaches a step function after a large number of steps of RG, i.e., at the fixed point. The critical point is at $g_c=0.804$. For $g<g_c$, the tensor belongs to the trivial phase while for $g>g_c$, the tensor belongs to the $\mathbb{Z}_2$ topological ordered phase.

Our algorithm can also be used to demonstrate the stability of topological order against local perturbation. As is shown in Ref. 75, local perturbations to the $\mathbb{Z}_2$ Hamiltonian correspond to variations in tensor that do not break the $\mathbb{Z}_2$ gauge symmetry. We picked tensors in the neighborhood of $T_{\mathbb{Z}_2}$ which preserve this gauge symmetry randomly and applied our renormalization algorithm (gauge symmetry is kept

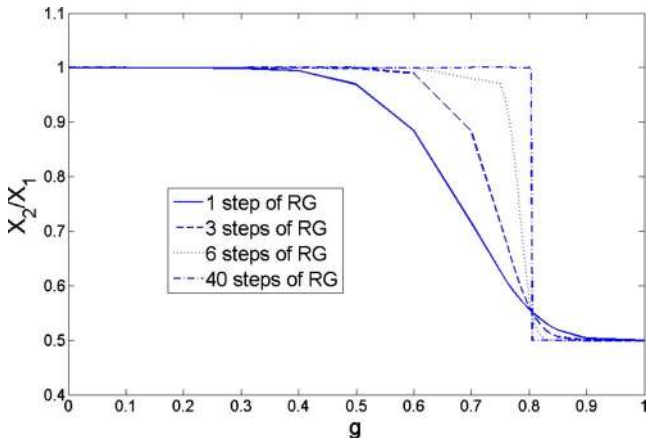

FIG. 22. (Color online) X_2/X_1 for tensors [Eq. (80)] under the renormalization flow. As the number of RG steps increases, the transition in X_2/X_1 becomes sharper and finally approaches a step function at fixed point. The critical point is at $g_c=0.804$.

throughout the renormalization process). We find that as long as the variation is small enough, the tensor flows back to $T_{\mathbb{Z}_2}$, up to a corner double line structure. This result shows that the $\mathbb{Z}_2$ topological ordered phase is stable against local perturbations.

XIII. SUMMARY

In this paper, we discuss a defining relation between local unitary transformation and quantum phases. We argue that two gapped states are related by a local unitary transformation if and only if the two states belong to the same quantum phase.

We can use the equivalent classes of local unitary transformations to define "patterns of long range entanglement." So the patterns of long-range entanglement correspond to universality classes of quantum phases, and are the essence of topological orders.[32]

As an application of this point of view of quantum phases and topological order, we use the generalized local unitary transformations to generate a wave function renormalization, where the wave functions flow within the same universality class of a quantum phase (or the same equivalent class of the local unitary transformations). In other words, the renormalization flow of a wave function does not change its topological order. Such a wave function renormalization allows us to classify topological orders, by classifying the fixed-point wave functions and the associated fixed-point local unitary transformations.

First, we find that the fixed-point local unitary transformations are described by the data $(N_{ijk}, F^{ijm,\alpha\beta}_{kln,\chi\delta}, P^{kj,\alpha\beta}_{i})$ that satisfy

$$N_{ijk} = N_{jki} = N_{k^*j^*i^*} \geq 0, \quad \sum_{j,k=0}^{N} N_{ii^*k} N_{jk^*j^*} \geq 1,$$

$$\sum_{m=0}^{N} N_{jim^*} N_{kml^*} = \sum_{n=0}^{N} N_{kjn^*} N_{l^*ni}, \tag{81}$$

$$(F^{ijm,\alpha\beta}_{kln,\chi\delta})^* = F^{jkn,\chi\delta}_{l^*i^*m^*,\beta\alpha},$$

$$\sum_{n,\chi,\delta} F^{ijm',\alpha'\beta'}_{kln,\chi\delta} (F^{ijm,\alpha\beta}_{kln,\chi\delta})^* = \delta_{m\alpha\beta,m'\alpha'\beta'},$$

$$\sum_{t} \sum_{\eta=1}^{N_{kjt^*}} \sum_{\varphi=1}^{N_{tin^*}} \sum_{\kappa=1}^{N_{lts^*}} F^{ijm,\alpha\beta}_{knt,\eta\varphi} F^{itn,\varphi\chi}_{lps,\kappa\gamma} F^{jkt,\eta\kappa}_{lsq,\delta\phi} = e^{i\theta_F} \sum_{\epsilon=1}^{N_{qmp^*}} F^{mkn,\beta\chi}_{lpq,\delta\epsilon} F^{ijm,\alpha\epsilon}_{qps,\phi\gamma}, \tag{82}$$

$$e^{i\theta_{P1}} P^{kj,\alpha\beta}_{i} = \sum_{m,\lambda,\gamma,l,\nu,\mu} F^{jj^*k,\beta\alpha}_{i^*i^*m^*,\lambda\gamma} F^{i^*mj,\lambda\gamma}_{m^*i^*l,\nu\mu} P^{lm,\mu\nu}_{i^*},$$

$$e^{i\theta_{P2}} P^{jp,\alpha\eta}_{i} \delta_{im} \delta_{\beta\delta} = \sum_{\chi=1}^{N_{kjk^*}} F^{ijm,\alpha\beta}_{klk,\chi\delta} P^{jp,\chi\eta}_{k^*}$$

$$\text{for all } k,i,l \text{ satisfying } N_{kil^*} > 0 \tag{83}$$

[see Eqs. (9), (12), (18), (23), (30), (33), (36), and (47)]. From the data $(N_{ijk}, F^{ijm,\alpha\beta}_{kln,\chi\delta}, P^{kj,\alpha\beta}_{i})$ we can further find out the fixed-point wave function by solving the following equations for $A^i, i=0,\ldots,N$:

$$A^i = e^{i\theta_A} A^{i^*} \neq 0, \quad \sum_i A^i (A^i)^* = 1,$$

$$P^{mj,\gamma\lambda}_{i} A^i = e^{i\theta_{A1}} P^{m^*i^*,\lambda\gamma}_{j^*} A^j,$$

$$\Phi^{\theta}_{ikj,\alpha\beta} = e^{i\theta'} \sum_{m,\lambda,\gamma} F^{ijk^*,\alpha\beta}_{j^*im,\lambda\gamma} P^{mj,\gamma\lambda}_{i} A^i,$$

$$\Phi^{\theta}_{ikj,\alpha\beta} = e^{i\theta_{A1}} \Phi^{\theta}_{kji,\alpha\beta},$$

$$\Phi^{\theta}_{ikj,\alpha\beta} = 0, \quad \text{if } N_{ikj} = 0,$$

$$\det(\Phi^{\theta}_{ikj,\alpha\beta}) \neq 0 \tag{84}$$

[see Eqs. (38), (40), (42), and (44)–(46)].

The combined data $(N_{ijk}, F^{ijm,\alpha\beta}_{kln,\chi\delta}, P^{kj,\alpha\beta}_{i}, A^i)$ that satisfy the conditions [Eqs. (81)–(84)] classify a large class of topological orders. We see that the problem of classifying a large class of topological orders becomes the problem of solving a set of nonlinear algebraic equations [Eqs. (81)–(84)].

The combined data $(N_{ijk}, F^{ijm,\alpha\beta}_{kln,\chi\delta}, P^{kj,\alpha\beta}_{i}, A^i)$ that satisfy the conditions [Eqs. (81)–(84)] also classify a large class of time-reversal invariant topological orders, if we restrict ourselves to real solutions. The solutions related by local orthogonal transformations all belong to the same phase since the local orthogonal transformations always connect to identity if we enlarge the Hilbert space.

We like to point out that we cannot claim that the solutions $(N_{ijk}, F^{ijm,\alpha\beta}_{kln,\chi\delta}, P^{kj,\alpha\beta}_{i}, A^i)$ classify all topological orders since we have assumed that the fixed-point local unitary transformations are described by tensors of finite dimensions. It appears that chiral topological orders, such as quantum Hall states, are described by tensors of infinite dimensions.

We note that the data $(N_{ijk}, F^{ijm,\alpha\beta}_{kln,\chi\delta}, P^{kj,\alpha\beta}_{i}, A^{i})$ just characterize different fixed-point wave functions. It is not guaranteed that the different data will represent different topological orders. However, for the simple solutions discussed in this paper, they all coincide with string-net states, where the topological properties, such as the ground-state degeneracy, number of quasiparticle types, the quasiparticle statistics, etc., were calculated from the data. From those topological properties, we know that those different simple solutions represent different topological orders. Also $(F^{ijm,\alpha\beta}_{kln,\chi\delta}, P^{kj,\alpha\beta}_{i}, A^{i})$ are real for the simple solutions discussed here. Thus they also represent topological orders with time-reversal symmetry. (Certainly, at the same time, they represent stable topological orders even without time-reversal symmetry.)

We also like to point out that our description of fixed-point local unitary transformations is very similar to the description of string-net states. However, the conditions [Eqs. (81)–(84)] on the data appear to be weaker than (or equivalent to) those[63] on the string-net data. So the fixed-point wave functions discussed in this paper may include all the string-net states (in 2D).

Last, we present a wave function renormalization scheme, based on the gLU transformations for generic TPS. Such a wave function renormalization always flows within the same phase (or within the same equivalence class of LU transformations). It allows us to determine which phase a generic TPS belongs to by studying the resulting fixed-point wave functions. We demonstrated the effectiveness of our method for both symmetry-breaking phases and topological ordered phases. We find that we can even use tensors that do not break symmetry to describe spontaneous symmetry-breaking states: if a state described by a symmetric tensor has a spontaneous symmetry breaking, the symmetric tensor will flow to a fixed-point tensor that has a form of direct sum.

ACKNOWLEDGMENTS

We would like to thank I. Chuang, M. Hastings, M. Levin, F. Verstraete, Z.-H. Wang, Y.-S. Wu, and S. Bravyi for some very helpful discussions. X.G.W. is supported by NSF under Grant No. DMR-0706078. Z.C.G. is supported in part by the NSF under Grant No. NSFPHY05-51164.

APPENDIX: EQUIVALENCE RELATION BETWEEN QUANTUM STATES IN THE SAME PHASE

In Secs. III and IV, we argued about the equivalence relation between gapped quantum ground states in the same phase. We concluded that two states are in the same phase if and only if they can be connected by local unitary evolution or constant depth quantum circuit,

$$|\Phi(1)\rangle \sim |\Phi(0)\rangle \quad \text{iff} \quad |\Phi(1)\rangle = \mathcal{T}\left[e^{-i\int_0^1 dg \tilde{H}(g)}\right]|\Phi(0)\rangle,$$

$$|\Phi(1)\rangle \sim |\Phi(0)\rangle \quad \text{iff} \quad |\Phi(1)\rangle = U^{M}_{circ}|\Phi(0)\rangle.$$

Now we want to make these arguments more rigorous, by stating clearly what is proved and what is conjectured, and by giving precise definition of two states being the same, the locality of operators, etc. We will show the equivalence in the following steps: (1) if two gapped ground states are in the same phase, then they are connected by local unitary evolution, (2) a gapped ground state remains in the same phase under local unitary evolution, and (3) a local unitary evolution can be simulated by a constant depth quantum circuit and vice versa. (All these discussions can be generalized to the case where the system has certain symmetries. $\tilde{H}(g)$ and U_{circ} used in the equivalence relation will then have the same symmetry as the system Hamiltonian H.)

First, according to the definition in Sec. III, two states $|\Phi(0)\rangle$ and $|\Phi(1)\rangle$ are in the same phase if we can find a family of local Hamiltonians $H(g)$, $g \in [0,1]$ with $|\Phi(g)\rangle$ being its ground state such that the ground-state average of any local operator O, $\langle\Phi(g)|O|\Phi(g)\rangle$ changes smoothly from $g=0$ to $g=1$. Here we allow a more general notion of locality for the Hamiltonian[34] and require $H(g)$ to be a sum of local operators $H_Z(g)$,

$$H(g) = \sum_{Z\in\mathcal{Z}} H_Z(g), \tag{A1}$$

where $H_Z(g)$ is a Hermitian operator defined on a compact region Z. $\Sigma_{Z\in\mathcal{Z}}$ sums over a set $\mathcal{Z}$ of regions. The set $\mathcal{Z}$ contains regions that differ by translations. The set $\mathcal{Z}$ also contains regions with different sizes. However, $H_Z(g)$ approaches zero exponentially as the size of the region Z approaches infinity. Or more precisely, for all sites u in the lattice

$$\sum_{Z\in\mathcal{Z},Z\ni u} \|H_Z(g)\||Z|\exp[\mu \mathrm{diam}(Z)] = O(1) \tag{A2}$$

for some positive constant μ. Here $\Sigma_{Z\in\mathcal{Z},Z\ni u}$ sums over all regions in the set $\mathcal{Z}$ that cover the site u, $\|\cdots\|$ denotes operator norm, $|Z|$ is the cardinality of Z, and $\mathrm{diam}(Z)$ is the diameter of Z. Therefore, instead of being exactly zero outside of a finite region, the interaction terms can have an exponentially decaying tail.

If $|\Phi(0)\rangle$ and $|\Phi(1)\rangle$ are gapped ground states of $H(0)$ and $H(1)$, then we assume that for all $\langle\Phi(g)|O|\Phi(g)\rangle$ to be smooth, $H(g)$ must remain gapped for all g. If $H(g)$ closes gap for some g_c, then there must exist a local operator O such that $\langle\Phi(g)|O|\Phi(g)\rangle$ has a singularity at g_c. We call the gapped $H(g)$ an adiabatic connection between two states in the same phase.

The existence of an adiabatic connection gives rise to a local unitary evolution between $|\Phi(0)\rangle$ and $|\Phi(1)\rangle$. A slight modification of Lemma 7.1 in Ref. 34 gives theorem 1 which is given below.

Theorem 1. Let $H(g)$ be a differentiable family of local Hamiltonians and $|\Phi(g)\rangle$ be its ground state. If the excitation gap above $|\Phi(g)\rangle$ is larger than some finite value Δ for all g, then we can define $\tilde{H}(g)=i\int dt F(t)\exp[iH(g)t][\partial_g H(g)]\exp[-iH(g)t]$, such that $|\Phi(1)\rangle=\mathcal{T}[e^{-i\int_0^1 dg\tilde{H}(g)}]|\Phi(0)\rangle$, where $F(t)$ is a function which has the following properties: (1) the fourier transform of $F(t)$, $\tilde{F}(\omega)$ is equal to $-1/\omega$ for $|\omega|>\Delta$. (2) $\tilde{F}(\omega)$ is infinitely differentiable. (3) $F(t)=-F(-t)$. Under this definition, $\tilde{H}(g)$ is local (almost) and satisfies

$$\|[\tilde{H}_Z(g),O_B]\| \le h'[\mathrm{dist}(Z,B)]|Z|\|\tilde{H}_Z(g)\|\|O_B\|, \quad \text{(A3)}$$

where O_B is any operator supported on site B, $\mathrm{dist}(Z,B)$ is the smallest distance between B and any site in Z, and $h'(l)$ is a function which decays faster than any negative power of l. $[\cdots]$ denotes commutator of two operators. This is called the quasiadiabatic continuation of states.

Therefore, we can show that if $|\Phi(0)\rangle$ and $|\Phi(1)\rangle$ are in the same phase, then we can find a local [as defined in Eq. (87)] Hamiltonian $\tilde{H}_Z(g)$ such that $|\Phi(1)\rangle = \mathcal{T}[e^{-i\int_0^1 dg\tilde{H}(g)}]|\Phi(0)\rangle$. In other words, states in the same phase are equivalent under local unitary evolution.

Note that here we map $|\Phi(0)\rangle$ exactly to $|\Phi(1)\rangle$. There is another version of quasiadiabatic continuation,[35] where the mapping is approximate. In that case, $\tilde{H}_Z(g)$ can be defined to have only exponentially small tail outside of a finite region instead of a tail which decays faster than any negative power. $\mathcal{T}[e^{-i\int_0^1 dg\tilde{H}(g)}]|\Phi(0)\rangle$ will not be exactly the same as $|\Phi(1)\rangle$ but any local measurement on them will give approximately the same result.

Next we want to show that the reverse is also true. Suppose that $|\Phi(0)\rangle$ is the gapped ground state of a local Hamiltonian $H(0)$, $H(0)=\Sigma_Z H_Z(0)$ and each $H_Z(0)$ is supported on a finite region Z. Apply a local unitary evolution generated by $\tilde{H}(s)$ to $|\Phi(0)\rangle$ and take it to $|\Phi(g)\rangle$, $g=0\sim 1$, $|\Phi(g)\rangle = U_g|\Phi(0)\rangle$, where $U_g=\mathcal{T}[e^{-i\int_0^g ds\tilde{H}(s)}]$. $|\Phi(g)\rangle$ is then ground state of $H(g)=U_gH(0)U_g^\dagger=\Sigma_Z U_g H_Z(0)U_g^\dagger=\Sigma_Z H_Z(g)$. Under unitary transformation U_g the spectrum of $H(0)$ does not change, therefore $H(g)$ remains gapped. To show that $H(g)$ also remains local, we use the Lieb-Robinson bound derived in Ref. 34, which gives

$$\begin{aligned}\|[H_Z(g),O_B]\| &= \|[U_gH_Z(0)U_g^\dagger,O_B]\| \\ &\le h[\mathrm{dist}(Z,B)]|Z|\|H_Z(0)\|\|O_B\|,\end{aligned}$$

where $h(l)$ decays faster than any negative power of l. Therefore, $H_Z(g)$ remains local up to a tail which decays faster than any negative power. $H(g)$ then forms a local gapped adiabatic connection between $|\Phi(0)\rangle$ and $|\Phi(1)\rangle$.

To detect for phase transition, we must check whether the ground-state average value of any local operator O, $\langle\Phi(g)|O|\Phi(g)\rangle$, has a singularity or not. $\langle\Phi(g)|O|\Phi(g)\rangle = \langle\Phi(0)|U_g^\dagger O U_g|\Phi(0)\rangle$. Using the Lieb-Robinson bound given in Ref. 34, we find $U_g^\dagger O U_g$ remains local [in the sense of Eq. (87)] and evolves smoothly with g. Therefore, $\langle\Phi(g)|O|\Phi(g)\rangle$ changes smoothly. In fact, because $H(g)$ is differentiable, the derivative of $\langle\Phi(g)|O|\Phi(g)\rangle$ to any order always exists. Therefore, there is no singularity in the ground-state average value of any local operator O and $|\Phi(0)\rangle$ and $|\Phi(1)\rangle$ are in the same phase. We have hence shown that states connected with local unitary evolution are in the same phase.

This completes the equivalence relation stated in (1). The definition of locality is slightly different in different cases, so there is still some gap in the equivalence relation. However, we believe that the equivalence relation should be valid with a slight generalization of the definition of locality.

Lastly, we want to show that the equivalence relation is still valid if we use constant depth quantum circuit instead of local unitary evolution. This is true because we can always simulate a local unitary evolution using a constant depth quantum circuit and vice versa.

To simulate a local unitary evolution of the form $\mathcal{T}[e^{-i\int_0^1 dg\tilde{H}(g)}]$, first divide the total time into small segments δt such that $\mathcal{T}[e^{-i\int_{m\delta t}^{(m+1)\delta t} dg\tilde{H}(g)}] \simeq e^{-i\delta t H(m\delta t)}$. $H(m\delta t) = \Sigma_Z H_Z(m\delta t)$. The set of local operators $\{H_Z(m\delta t)\}$ can always be divided into a finite number of subsets $\{H_{Z_1^i}(m\delta t)\}$, $\{H_{Z_2^i}(m\delta t)\}\cdots$ such that elements in the same subset commute with each other. Then we can do Trotter expansion and approximate $e^{-i\delta t H(m\delta t)}$ as $e^{-i\delta t H(m\delta t)} \simeq (U^{(1)}U^{(2)}\cdots)^n$, where $U^{(1)}=\Pi_i e^{-i\delta t H_{Z_1^i}/n}$, $U^{(2)}=\Pi_i e^{-i\delta t H_{Z_2^i}/n}\cdots$ Each term in $U^{(1)}$, $U^{(2)}$ commute, therefore they can be implement as a piecewise local unitary operator. Putting these piecewise local unitary operators together, we have a quantum circuit which simulates the local unitary evolution. The depth of circuit is proportional to $n\times(1/\delta t)$. It can be shown that to achieve a simulation with constant error, a constant depth circuit would suffice.[76]

On the other hand, to simulate a constant depth quantum circuit $U_{circ}=U_{pwl}^{(1)}U_{pwl}^{(2)}\cdots U_{pwl}^{(2)}$, where $U_{pwl}^{(k)}=\Pi_i U_i^{(k)}$ with a local unitary evolution, we can define the time-dependent Hamiltonian as $H(t)=\Sigma_i H_i^{(k)}$, such that for $(k-1)\delta t < t < k\delta t$, $e^{iH_i^{(k)}\delta t}=U_i^{(k)}$. It is easy to check that $\mathcal{T}[e^{-i\int_0^{M\delta t} dg\tilde{H}(g)}]=U_{circ}$. The simulation time needed is $M\delta t$. We can always choose a finite δt such that $\|H_i^{(k)}\|$ is finite and the evolution time is finite.

We have shown that constant depth quantum circuit and local unitary evolution can simulate each other. The equivalence relation [Eq. (1)] can therefore also be stated in terms of constant depth circuit as in Eq. (4).

[1] L. D. Landau, Phys. Z. Sowjetunion **11**, 26 (1937).

[2] V. L. Ginzburg and L. D. Landau, Zh. Eksp. Teor. Fiz. **20**, 1064 (1950).

[3] J. G. Bednorz and K. A. Mueller, Z. Phys. B: Condens. Matter **64**, 189 (1986).

[4] P. W. Anderson, Science **235**, 1196 (1987).

[5] G. Baskaran, Z. Zou, and P. W. Anderson, Solid State Commun. **63**, 973 (1987).

[6] I. Affleck and J. B. Marston, Phys. Rev. B **37**, 3774 (1988).

[7] D. S. Rokhsar and S. A. Kivelson, Phys. Rev. Lett. **61**, 2376 (1988).

[8] I. Affleck, Z. Zou, T. Hsu, and P. W. Anderson, Phys. Rev. B **38**, 745 (1988).

[9] E. Dagotto, E. Fradkin, and A. Moreo, Phys. Rev. B **38**, 2926 (1988).

[10] V. Kalmeyer and R. B. Laughlin, Phys. Rev. Lett. **59**, 2095

(1987).
[11] X.-G. Wen, F. Wilczek, and A. Zee, Phys. Rev. B **39**, 11413 (1989).
[12] X.-G. Wen, Phys. Rev. B **40**, 7387 (1989).
[13] X.-G. Wen, Int. J. Mod. Phys. B **4**, 239 (1990).
[14] The name "topological order" is motivated by the low-energy effective theory of the chiral spin states, which is a topological quantum field theory (Ref. 77).
[15] X.-G. Wen, Phys. Rev. B **43**, 11025 (1991).
[16] A. Kitaev and J. Preskill, Phys. Rev. Lett. **96**, 110404 (2006).
[17] M. Levin and X.-G. Wen, Phys. Rev. Lett. **96**, 110405 (2006).
[18] J. B. Marston and I. Affleck, Phys. Rev. B **39**, 11538 (1989).
[19] X.-G. Wen, Phys. Rev. Lett. **66**, 802 (1991).
[20] A. Y. Kitaev, Ann. Phys. (N.Y.) **321**, 2 (2006).
[21] X.-G. Wen and Q. Niu, Phys. Rev. B **41**, 9377 (1990).
[22] F. D. M. Haldane and E. H. Rezayi, Phys. Rev. B **31**, 2529 (1985).
[23] G. Kotliar and J. Liu, Phys. Rev. B **38**, 5142 (1988).
[24] N. Read and S. Sachdev, Phys. Rev. Lett. **66**, 1773 (1991).
[25] X.-G. Wen, Phys. Rev. B **44**, 2664 (1991).
[26] P. A. Lee and N. Nagaosa, Phys. Rev. B **46**, 5621 (1992).
[27] A. Y. Kitaev, Ann. Phys. (N.Y.) **303**, 2 (2003).
[28] W. Rantner and X.-G. Wen, Phys. Rev. B **66**, 144501 (2002).
[29] M. Hermele, T. Senthil, M. P. A. Fisher, P. A. Lee, N. Nagaosa, and X.-G. Wen, Phys. Rev. B **70**, 214437 (2004).
[30] X.-G. Wen, Phys. Rev. B **65**, 165113 (2002).
[31] X.-G. Wen and A. Zee, Phys. Rev. B **66**, 235110 (2002).
[32] X.-G. Wen, Phys. Lett. A **300**, 175 (2002).
[33] The conjecture is for symmetry-breaking states with finite energy gaps. However, it is unclear whether it is possible to find a definition of "short-range quantum entanglement" to make the conjecture valid for gapless symmetry-breaking states.
[34] S. Bravyi, M. Hastings, and S. Michalakis, J. Math. Phys. **51**, 093512 (2010).
[35] M. B. Hastings and X.-G. Wen, Phys. Rev. B **72**, 045141 (2005).
[36] For each Hamiltonian, we can introduce an algebra of local operators. If the energy gap for $H(g)$ is finite for all g in the segment [0,1], Ref. 35 shows that the algebra of local operators for different g's are isomorphic to each other at low energies, using a quasiadiabatic continuation of quantum states.
[37] E. H. Lieb and D. W. Robinson, Commun. Math. Phys. **28**, 251 (1972).
[38] S. Bravyi, M. B. Hastings, and F. Verstraete, Phys. Rev. Lett. **97**, 050401 (2006).
[39] D. I. Tsomokos, A. Hamma, W. Zhang, S. Haas, and R. Fazio, Phys. Rev. A **80**, 060302 (2009).
[40] A state is called a gapped state if there exist a local Hamiltonian such that the state is the gapped ground state of the Hamiltonian.
[41] Z.-C. Gu and X.-G. Wen, Phys. Rev. B **80**, 155131 (2009).
[42] F. Verstraete, J. I. Cirac, J. I. Latorre, E. Rico, and M. M. Wolf, Phys. Rev. Lett. **94**, 140601 (2005).
[43] G. Vidal, Phys. Rev. Lett. **99**, 220405 (2007); *Understanding Quantum Phase Transitions*, edited by L. D. Carr (Taylor & Francis, Boca Raton, 2010)).
[44] S. Bravyi (personal communication); B. Yoshida, arXiv:1007.4601 (unpublished).
[45] F. D. M. Haldane, Phys. Lett. A **93**, 464 (1983).
[46] F. Pollmann, E. Berg, A. Turner, and M. Oshikawa, arXiv:0909.4059 (unpublished).
[47] C. L. Kane and E. J. Mele, Phys. Rev. Lett. **95**, 226801 (2005).
[48] B. A. Bernevig and S.-C. Zhang, Phys. Rev. Lett. **96**, 106802 (2006).
[49] C. L. Kane and E. J. Mele, Phys. Rev. Lett. **95**, 146802 (2005).
[50] J. Moore and L. Balents, Phys. Rev. B **75**, 121306(R) (2007).
[51] L. Fu, C. L. Kane, and E. J. Mele, Phys. Rev. Lett. **98**, 106803 (2007).
[52] X.-L. Qi, T. L. Hughes, and S.—C. Zhang, Phys. Rev. B **78**, 195424 (2008).
[53] N. Read and D. Green, Phys. Rev. B **61**, 10267 (2000).
[54] W.-H. Ko, P. A. Lee, and X.-G. Wen, Phys. Rev. B **79**, 214502 (2009).
[55] S.-P. Kou, M. Levin, and X.-G. Wen, Phys. Rev. B **78**, 155134 (2008).
[56] S.-P. Kou and X.-G. Wen, Phys. Rev. B **80**, 224406 (2009).
[57] S. Raghu, X.-L. Qi, C. Honerkamp, and S.-C. Zhang, Phys. Rev. Lett. **100**, 156401 (2008).
[58] Y. Zhang, Y. Ran, and A. Vishwanath, Phys. Rev. B **79**, 245331 (2009).
[59] D. Pesin and L. Balents, Nat. Phys. **6**, 376 (2010).
[60] B. Yang and Y. Kim, Phys. Rev. B **82**, 085111 (2010).
[61] J. Maciejko, X. Qi, A. Karch, and S. Zhang, arXiv:1004.3628 (unpublished).
[62] B. Swingle, M. Barkeshli, J. McGreevy, and T. Senthil, arXiv:1005.1076 (unpublished).
[63] M. A. Levin and X.-G. Wen, Phys. Rev. B **71**, 045110 (2005).
[64] M. Aguado and G. Vidal, Phys. Rev. Lett. **100**, 070404 (2008); R. König, B. W. Reichardt, and G. Vidal, Phys. Rev. B **79**, 195123 (2009).
[65] S. Hong, arXiv:0907.2204 (unpublished).
[66] M. Freedman, C. Nayak, K. Shtengel, K. Walker, and Z. Wang, Ann. Phys. (N.Y.) **310**, 428 (2004).
[67] A. Gendiar, N. Maeshima, and T. Nishino, Prog. Theor. Phys. **110**, 691 (2003).
[68] Y. Nishio, N. Maeshima, A. Gendiar, and T. Nishino, arXiv:cond-mat/0401115 (unpublished).
[69] N. Maeshima, J. Phys. Soc. Jpn. **73**, 60 (2004).
[70] F. Verstraete and J. Cirac, arXiv:cond-mat/0407066 (unpublished).
[71] F. Verstraete, J. I. Cirac, and V. Murg, Adv. Phys. **57**, 143 (2008).
[72] Z.-C. Gu, M. Levin, and X.-G. Wen, Phys. Rev. B **78**, 205116 (2008).
[73] H. C. Jiang, Z. Y. Weng, and T. Xiang, Phys. Rev. Lett. **101**, 090603 (2008).
[74] M. Levin and C. P. Nave, Phys. Rev. Lett. **99**, 120601 (2007).
[75] X. Chen, B. Zeng, Z. Gu, I. Chuang, and X. Wen, arXiv:1003.1774 (unpublished).
[76] S. Lloyd, Science **273**, 1073 (1996).
[77] E. Witten, Commun. Math. Phys. **121**, 351 (1989).